



NTNU – Trondheim
Norwegian University of
Science and Technology

Simulation of the natural frequencies in a pump-turbine runner in air and water

Øyvind Moen Fjeld

Master of Energy and Environmental Engineering

Submission date: June 2015

Supervisor: Torbjørn Kristian Nielsen, EPT

Norwegian University of Science and Technology
Department of Energy and Process Engineering

EPT-M-2015-22

MASTEROPPGAVE

for

Student Øyvind Moen Fjeld

Våren 2015

Simulering av egenfrekvenser til sirkulær disk i luft og vann

*Simulation of natural frequencies in a circular disc in air and water***Bakgrunn og målsetting**

Mange Francisturbiner i Norge er modne for utskifting etter å ha vært i drift i nærmere femti år. Flere Francisturbiner som har fått nye og «moderne» løpehjul har opplevd problemer knyttet til utmatting og skovlbrudd. Disse problemene tror man er grunnet at egenfrekvenser i løpehjulene har blitt for nære frekvenser som dukker opp under drift og man har kommet nærmere å få resonans i løpehjulene. For enkle strukturer er det relativt lett å regne seg frem til strukturens egenfrekvenser. Når strukturene blir såpass komplekse som er Francis løpehjul som i tillegg er fylt med vann omringet av tynne sjikt med vann mot andre faste flater viser det seg mye vanskeligere å regne på, og teori stemmer ikke godt nok med praksis. Det er behov for å kunne bestemme egenfrekvensen til slike komplekse strukturer og dette behovet stammer fra ønsket om å kunne konstruere nye løpehjul som vil ha egenskaper som gir problemfri drift i nye femti år.

Simuleringsverktøy for å beregne egenfrekvenser benytter seg av modeller som i større eller mindre grad representerer den fysiske verden på en nøyaktig nok måte. Å validere resultat fra simuleringsverktøy mot eksperimentelle resultat blir derfor ekstra utfordrende, og faren er at en dårlig måling verifiserer en uriktig modell. Man bør derfor være sikker på at modellen man benytter seg av er anvendbar på problemet.

Oppgaven bearbeides ut fra følgende punkter

- 1 Litteratursøk angående strukturanalyse og strukturers egenfrekvenser
- 2 Spesielt sette seg inn i teorien omtalt som «Structural Acoustics» og avgjøre om dette er en god modell/metodikk for å bestemme egenfrekvensene til neddykkede strukturer
- 3 Simulere ved hjelp av valgt metodikk et modellløpehjul med fokus på å bestemme egenfrekvenser
- 4 Simulere ved hjelp av samme metodikk geometrien for modellløpehjulet bygd opp av dynamisk riktig skalert materiale for å finne egenfrekvensene og forskyvninger

” _ ”

Senest 14 dager etter utlevering av oppgaven skal kandidaten levere/sendte instituttet en detaljert fremdrift- og eventuelt forsøksplan for oppgaven til evaluering og eventuelt diskusjon med faglig ansvarlig/veiledere. Detaljer ved eventuell utførelse av dataprogrammer skal avtales nærmere i samråd med faglig ansvarlig.

Besvarelsen redigeres mest mulig som en forskningsrapport med et sammendrag både på norsk og engelsk, konklusjon, litteraturliste, innholdsfortegnelse etc. Ved utarbeidelsen av teksten skal kandidaten legge vekt på å gjøre teksten oversiktlig og velskrevet. Med henblikk på lesning av besvarelsen er det viktig at de nødvendige henvisninger for korresponderende steder i tekst, tabeller og figurer anføres på begge steder. Ved bedømmelsen legges det stor vekt på at resultatene er grundig bearbeidet, at de oppstilles tabellarisk og/eller grafisk på en oversiktlig måte, og at de er diskutert utførlig.

Alle benyttede kilder, også muntlige opplysninger, skal oppgis på fullstendig måte. For tidsskrifter og bøker oppgis forfatter, tittel, årgang, sidetall og eventuelt figurnummer.

Det forutsettes at kandidaten tar initiativ til og holder nødvendig kontakt med faglærer og veileder(e). Kandidaten skal rette seg etter de reglementer og retningslinjer som gjelder ved alle (andre) fagmiljøer som kandidaten har kontakt med gjennom sin utførelse av oppgaven, samt etter eventuelle pålegg fra Institutt for energi- og prosesssteknikk.

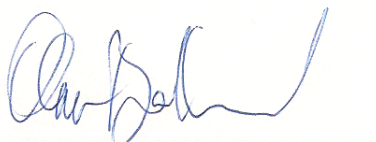
Risikovurdering av kandidatens arbeid skal gjennomføres i henhold til instituttets prosedyrer. Risikovurderingen skal dokumenteres og inngå som del av besvarelsen. Hendelser relatert til kandidatens arbeid med uheldig innvirkning på helse, miljø eller sikkerhet, skal dokumenteres og inngå som en del av besvarelsen. Hvis dokumentasjonen på risikovurderingen utgjør veldig mange sider, leveres den fulle versjonen elektronisk til veileder og et utdrag inkluderes i besvarelsen.

I henhold til "Utfyllende regler til studieforskriften for teknologistudiet/sivilingeniørstudiet" ved NTNU § 20, forbeholder instituttet seg retten til å benytte alle resultater og data til undervisnings- og forskningsformål, samt til fremtidige publikasjoner.

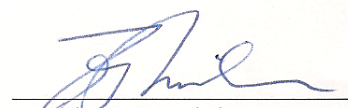
Besvarelsen leveres digitalt i DAIM. Et faglig sammendrag med oppgavens tittel, kandidatens navn, veileders navn, årstall, instituttnavn, og NTNUs logo og navn, leveres til instituttet som en separat pdf-fil. Etter avtale leveres besvarelse og evt. annet materiale til veileder i digitalt format.

- Arbeid i laboratorium (vannkraftlaboratoriet, strømmingsteknisk, varmeteknisk)
- Feltarbeid

NTNU, Institutt for energi- og prosesssteknikk, 14. januar 2015



Olav Bolland
Instituttleder



Torbjørn K. Nielsen
Faglig ansvarlig/veileder

Medveileder: Pål-Tore Storli, Vannkraftlaboratoriet

PREFACE

This Master thesis was written for the Water Power Laboratory, Department of Energy and Process Engineering (EPT) at NTNU during the spring of 2015. The problem description was made on the basis of my project thesis. Working with natural frequencies of structures has been interesting and challenging.

I would like to thank Torbjørn K. Nielsen for sharing his knowledge and experience. Thanks to Frode Kristoffer Amundsen Kjøsnes for the collaboration during the last months. A special thanks to Einar Agnalt which was very helpful solving problems with the CAD geometry.

Øyvind Moen Fjeld

Trondheim, 17.06.2015

ABSTRACT

Structural-acoustic models are used in the industry to determine the natural frequencies of runners and impellers in hydraulic turbomachinery under construction of the machines. The structural-acoustic models have to be able to handle the complex boundary conditions and loads experienced. The new trends in water power production have led to new operating regimes for several hydro power plants. More time is spent outside Best Efficiency Point (BEP) and frequent adjustment of output is common. These factors put large stresses on the structure. Especially for high head turbines where forces are high, fatigue loads could cause serious damage after short time of operation. The fatigue loads are amplified if they get into resonance with the natural frequency of the runner. Knowledge of the natural frequencies of a turbine are therefore of great importance. Structural-acoustic models of the turbine and its surroundings have become an important part of construction to maximize efficiency and safety. Over the last decade several breakdowns of newly installed turbines have shown that there are challenges to overcome in design, building and operation of these turbomachines. In this report, a CAD model of a pump-turbine runner is used in numerical simulations to investigate its structural behavior and natural frequencies in air and submerged in water. The goal is to find the added mass effect and see how well numerical simulations match experiments done on the exact same pump-turbine runner at the Water Power Laboratory at NTNU. ANSYS Mechanical software is used for the simulations. The results obtained in modal analysis showed a Frequency Reduction Ratio (FRR) in water between 14-34 %, depending on the mode shape. FRR in the harmonic response analysis showed values from 11-20 %. Comparison with the experimental investigation showed large deviations for all modes except (2,0).

SAMMENDRAG

Strukturanalyse med akustiske modeller blir brukt i industrien for å bestemme egenfrekvensene til vann-turbiner. Modellen som blir brukt under simuleringene må være kapabel til å håndtere de kompliserte grensebetingelsene og kreftene som er involvert. Nye trender innen vannkraftproduksjon har ført til nye produksjonsmønstre. Større del av produksjonstiden blir tilbrakt utenfor punktet for optimal virkningsgrad og store svingninger i produksjonen er vanlig. Disse faktorene fører til store belastninger på turbinen. Spesielt for høytrykksmaskiner, der kreftene er store, kan trykkpulsasjoner føre til store skader etter kort tid. Trykkpulsasjonene blir forsterket hvis de kommer i resonans med egenfrekvensene til turbinen. På bakgrunn av dette er det viktig å ha kunnskap om egenfrekvensene til turbinen. Strukturanalyse med akustiske modeller av turbinen og omgivelsene har utviklet seg til å bli en stor del av produksjonsprosessen for å øke effektiviteten og sikkerheten. Over de siste tiårene har flere tretthetsbrudd i nylig installerte turbiner vist at det er utfordringer å overkomme i design og produksjonsprosessen. I denne rapporten blir en CAD model av en pumpe-turbin brukt i numeriske simuleringer for å undersøke bevegelsene og egenfrekvensene i luft og i vann. Målet er å finne frekvensreduksjonen forårsaket av ekstra-masse effekten og se hvor godt numeriske simuleringer etterlikner eksperimenter på den samme pumpe-turbinen i Vannkraftlaboratoriet ved NTNU. ANSYS Mechanical programvare er brukt for å gjennomføre simuleringene. Resultatene funnet i modal analysen viser en frekvensreduksjon på mellom 14-34 %, avhengig av modalformen. Frekvensreduksjonen i harmonisk response analysen er på mellom 11-20 %. Sammenlikninger med eksperimentet viser store variasjoner for alle moder bortsett fra (2,0).

CONTENTS

Preface	i
Abstract	ii
Nomenclature	vii
1 Introduction	1
1.1 Trends in water power production	1
1.1.1 New operating regime	1
1.1.2 New building material and production regime	1
1.1.3 Higher loads	2
1.1.4 Computer simulations	2
2 Natural Frequency of structures	3
2.1 Resonance	4
2.2 Mode shapes	5
2.3 Excitation forces on turbines	7
2.3.1 Runner Frequency	7
2.3.2 Blade passing frequency	7
2.3.3 Guide vane frequency	7
3 Structural analysis	10
3.1 Finite Element Method	10
3.2 FEM in ANSYS	11
3.2.1 Modal Analysis	12
3.2.2 Harmonic response analysis	14
4 Structural acoustics	16
4.1 Fluid Solid Interaction	16
4.2 Fluid Elements	18
5 Previous work done on numerical simulations of submerged structures	21
6 Numerical simulations	22
7 Results and discussion	25
7.1 Modal analysis	25
7.2 Harmonic response analysis	26
7.3 Experiment	29
8 Conclusion	31
9 Further work	32
References	33

LIST OF FIGURES

1	Spring-mass system	3
2	Resonance	4
3	Tahoma bridge	5
4	Mode shapes of bar	6
5	Mode shapes of disk	6
6	Guide vane wakes	8
7	RSI	8
8	"Sea of springs"	10
9	Basics of FEM	11
10	Acoustic elements	19
11	Acoustic elements 2	19
12	FSI transfer matrix	20
13	Tetrahedral element	22
14	Turbine with surrounding fluid	23
15	Turbine and mesh	23
16	Comparison of frequencies in air and in water	25
17	FRR	26
18	Comparison of the frequency response in air and in water	27
19	Unidentified modes	29
20	Frequency plot from the experiment with the pump-turbine in air	30

LIST OF TABLES

1	Material properties of the bronze pump-turbine	22
2	Mesh info	23
3	Time consumption of the simulations	24
4	Pump-turbine specifications	24
5	Results from the modal analysis	25
6	Frequencies of modes from the harmonic response analysis	28
7	Deviations of frequencies between modal analysis and harmonic response in water	28
8	Experimental results of the pump-turbine in air	29

NOMENCLATURE

[C]	Structural damping matrix	
[K]	Structural stiffness matrix	
[L]	Lower triangular matrix	
[M]	Structural mass matrix	
[R]	Acoustic fluid boundary matrix	
[U]	Upper triangular matrix	
\vec{n}	outward normal unit vector of fluid domain	
{ \ddot{u} }	Nodal acceleration vector	
{ \dot{u} }	Nodal velocity vector	
{ F }	Load vector	
{ u }	Nodal displacement vector	
FS	Fluid-solid boundary	
k	Stiffness constant	N/m
c	speed of sound	m/s
Hz	Hertz	1/s
p	acoustic pressure	Pa
Q	mass source	m ³ /s
t	time	s
u	displacement	m

Greek Symbols

α	mass matrix multiplier	
β	stiffness matrix multiplier	
μ	dynamic viscosity	kg/ms
ω	Frequency	rad/s
Φ	Displacement potential	
ϕ	Displacement phase shift	rad/s
ρ	mean fluid density	kg/m ³
ζ	constant modal damping ratio	

Sub- and superscripts

F	Fluid
S	Solid
i	counter

img imaginary component
ma material
r real component

Acronyms

ACT Application Customization Toolkit
BEP Best Efficiency Point
FEM Finite Element Method
FRR Frequency Reduction Ratio
GUI Graphical User Interface
ODE Ordinary Differential Equation
PCG Preconditioned Conjugate Gradient
PDE Partial Differential Equation
RSI Rotor-Stator Interaction
CAD Computer-Aided Design
HR Harmonic Response analysis
MA Modal Analysis
RAM Random Access Memory

1 INTRODUCTION

Water power is one of the largest renewable energy sources in the world. It is highly recognized for its reliability and flexibility. The production is easy and fast to adjust and, when connected to a reservoir, long term planning of the production is possible. No other large renewable energy sources have this capability. In the recent years a gradual development of more renewable energy sources have changed the energy system. Especially wind and solar power have increased. These sources of energy are unreliable, because of their hour-to-hour weather dependency. This development increases the need of stable and reliable energy sources to stabilize the grid. Hydro power plants, with a reservoir, have the ability to produce power when its needed and thus can counterweight the contribution of the other energy sources. This will ensure that water power will play an important role in the energy system of tomorrow.

1.1 TRENDS IN WATER POWER PRODUCTION

New trends have altered the way water power turbines are built and operated. This has caused some challenges. In recent years several high head Francis and pump-turbines have experienced breakdowns after only a short time of operation. One example is Svartisen Powerplant in Norway [6]. The cause of the failures is thought to be high pressure pulsations, causing high stresses on the runner [15, 40]. The reason why these pulsations are getting dangerously high are not clearly understood. One explanation is resonance between the natural frequencies of the runner and one of the Rotor-Stator Interaction (RSI) frequencies [5]. No matter what is the reason for these breakdowns, they have become more frequent over the last decades. Recent trends in turbine manufacturing and operation seem to have made the turbines more vulnerable to fatigue damage.

1.1.1 NEW OPERATING REGIME

Historically turbines have been operated at, or near, Best Efficiency Point (BEP) and with small changes in water discharge and power output. This operating regime has altered and many of the turbines today are constantly adjusting the power output. A North American survey showed that hydro power units that originally had 100 start/stop sequences each year, had increased to a number of 500 over the last decade [9]. This is to a large extent caused by the introduction of more intermittent energy sources and better power grids [9]. In pump-turbine power plants the turbine is reversed in some periods, pumping water back up into the reservoir, further increasing the load on the machine. High pressure pulsations will often occur at part load or during start and stop. Operating at these conditions for longer periods of time will consequently increase the risk of high stresses on the runner and ultimately cause fatigue breakdowns.

1.1.2 NEW BUILDING MATERIAL AND PRODUCTION REGIME

Traditionally Francis turbines were produced using steel castings in the pressure carrying parts [1]. This made the turbines heavy, difficult to transport and very labour-intensive to make, but they were structurally solid. As the turbines increased in size and new materials and welding methods were developed, changes in the manufacturing process made the turbines easier and cheaper to build. Transport costs also decreased. The drawback of this development was that turbines gave less damping of pressure pulsations and had to be welded and put together with great care to minimize the risk of faults weakening the structure [1]. The result of these new materials and new production regime is a less robust turbine, which is more fragile to the fatigue loads experienced during operation. In addition, even if the turbine is strong, the damping ratio is low. This means that if excited at the right frequency, there are little damping to prevent high amplitudes from occurring.

1.1.3 HIGHER LOADS

In recent years many old power plants have been upgraded. To meet the requirements of today, an increase in the output and operating range of the turbines is desired. The total energy output over a year is decided by the amount of precipitation, not by the size of the runner, still power companies want to increase the output of the turbines to be able to produce more power when the prices are high and thus increase their revenue. To facilitate this, more water needs to flow through the power plant. Increasing pipe diameters is often difficult, labour intensive and expensive. Therefore increasing the velocity of the water is the preferred option. This increases the loads on the runner and the chance of fatigue damage.

1.1.4 COMPUTER SIMULATIONS

Pressure pulsations will increase if the frequency of the pulsations is close to the natural frequency of the runner. To be able to construct high head Francis turbines that avoids any resonance phenomena, knowledge of the natural frequency of the structure is important. Before the runner is built a dynamic analysis of the runner is vital to avoid problems during operation. The calculations are performed by computer programs using numerical methods, and require high computational resources to get accurate results. The computer simulations are gradually improving, at the same time is the margin for error decreasing because materials and operating conditions are pushed to maximize the revenue. Small deviations can have serious consequences. Even if the computer simulations are correct, the input of information to the computer model is another element of uncertainty. Which parts of the turbine that needs to be modelled, the necessity of modelling the flow of water and how to get the best possible mesh compatibility between fluid and structure on the interface, are only some of the questions to assess [37]. The number of breakdowns of newly installed turbines, likely caused by some sort of resonance in the runner, highlights the fact that there is something in the process that is not clearly understood.

Originally, the plan was to use a circular disk for the simulations in this report, but after discussions with my supervisor Torbjørn Nielsen and master student Frode Kristoffer Amundsen Kjøsnæs, which will perform similar experimental work at the Water Power Laboratory, a pump-turbine runner was yet chosen as the basis for the thesis. The reason for this choice is because a pump-turbine runner is closer to a real operating turbine than a circular disk and that CAD drawings of the turbine existed, making it possible to do numerical simulations on the same structure. The numerical simulations will try to replicate the experimental setup and make comparisons of the results possible. Yet first, a general view of the foundation of natural frequencies, resonance and pressure pulsations within a turbine are presented together with its implementation in ANSYS Mechanical Software. In Section 7, the results from the numerical simulations are presented and compared with experiments on the pump-turbine runner executed by Frode Kristoffer Amundsen Kjøsnæs at the Water Power Laboratory.

2 NATURAL FREQUENCY OF STRUCTURES

The natural frequency of a system is the frequency at which the system will oscillate when excited in absence of any driving or damping forces [14]. Figure 1 shows a simple spring-mass system. When put into motion it will oscillate at its natural frequency, which is a property of the system. Newton's second law of motion is the governing equation. When the spring-mass system is in its equilibrium position, the spring force pulling up equals the gravitational force pulling down.

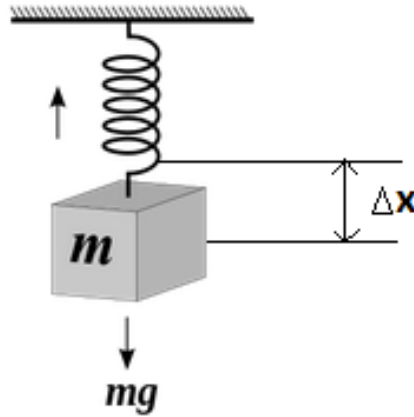


Figure 1: Spring-mass system

$$k\Delta x = mg \quad (1)$$

We can now use Newton's second law of motion:

$$m\ddot{x} = \sum F = mg - k(\Delta x + x) \quad (2)$$

because $k\Delta x = mg$, we obtain:

$$m\ddot{x} = -kx \quad (3)$$

By defining a frequency parameter

$$\omega^2 = \frac{k}{m} \quad (4)$$

Equation 3 can be written as

$$\ddot{x} + \omega^2 x = 0 \quad (5)$$

This equation is a homogeneous second order linear differential equation [36] and has the following solution:

$$x = A \sin \omega t + B \cos \omega t \quad (6)$$

A and B are two constants which can be evaluated from the initial conditions $x(0)$ and $\dot{x}(0)$. The natural frequency of the spring-mass system can then be found:

$$f = \frac{1}{2\pi} \sqrt{\frac{k}{m}} \quad (7)$$

The frequency of which the system tends to oscillate is only depending on the mass and stiffness. The same physics is the basic for all natural frequency calculation. When plucking a guitar string, the frequency of the vibrations is the natural frequency of the string. As an example, the A tone string on a guitar has a natural frequency of 440 Hz.

2.1 RESONANCE

When there is applied force, the frequency of this force has a great impact on the behavior of the system. If the applied force is close to its natural frequency, the energy will add up for every period. A simple example of this is a swing. Small pushes applied over time at the right frequency creates a large amplitude of motion, but if the same pushes are not synchronized with the natural frequency of the swing, no large amplitude will be achieved. In many applications resonance is important, for example in microwave ovens, lasers and musical instruments. In other areas resonance can be a problem. In many structural engineering situations avoiding resonance phenomena is crucial because of the dangerous build up of energy, which could ultimately cause failure and breakdowns. It could be high buildings, air plane wings or bridges (see Figure 3). To avoid resonance, knowledge of the natural frequency of the system is important. By knowing this frequency it is possible to make sure that the applied force not coincides with the frequency of the system. When it comes to water power turbines, having complicated boundary conditions and experiencing high loads at high frequencies, calculation of the natural frequencies can be difficult. In addition, as illustrated in Figure 2, the response of a system is not only a matter of keeping away from one frequency. Also frequencies close to the resonance frequency could induce higher pressure amplitudes. As a water turbine is experiencing a high number of load cycles (about 10^9 cycles per year) only small increases in these amplitudes could potentially be damaging.

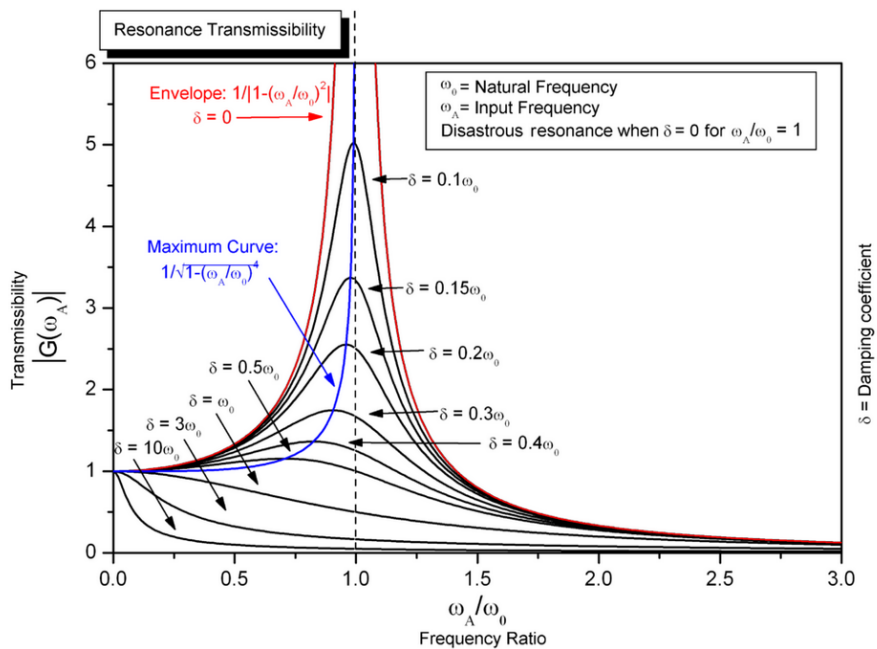


Figure 2: The response of a structure at the frequencies in and around resonance [25].



Figure 3: The Tahoma bridge in Washington, USA was brought down by wind gusts with the same frequency as the bridge natural frequency only months after opening [7].

2.2 MODE SHAPES

The vibration of a body can be split up into basic patterns or modes. To describe the movement of these modes each one is characterized by the number of nodal diameters and nodal circles. They are formed by the points on the object which remain stationary as it vibrates (see Figure 4). When a body vibrates the summation of each mode adds together to create the "total" vibration of the body. Each mode has its own frequency which, if excited by a force with the same frequency, could start resonating with increasingly higher amplitude. When impacting a structure with a range of frequencies some modes will at certain points respond more than others. The vibration of the body will at this frequency be dominated by the mode vibrating at its resonance frequency. This means that to avoid resonance in for instance water turbines, it is not enough to keep away from one frequency only. Each mode shape has its own frequency which can get into resonance with the applied force. The modes of a string have the special feature that all the modes are integer multiples of each other. The n^{th} mode has a frequency of n times the frequency of the first node [21]. However this is not the general feature of modes. A bar for instance does not follow this rule, as seen in Figure 4. Neither will more complex structures. The mode shape frequencies must be calculated separately for each structure.

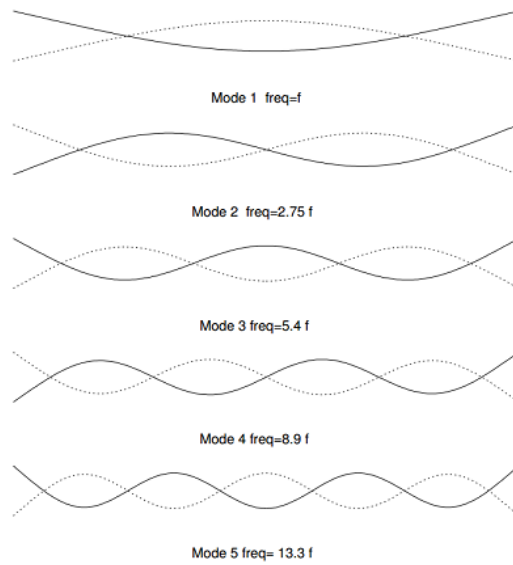


Figure 4: Mode shapes of a bar with 1 degree of freedom

Figure 4 shows the shape of the first 5 nodes of a vibrating bar (without twisting). Along the bar there are nodal points. These spots remain stationary as the bar vibrates. Detecting all vibrating modes can be difficult. If measuring the first 5 modes of the bar in Figure 4 with one sensor, placing it at approximately $1/4$ of the distance from one end of the bar, the first and the fifth mode will be difficult to detect because the deflection of these modes are small that close to the sensor [21]. The sensor is placed close to the modes nodal point. This shows the importance of correct sensor placement when measuring natural frequencies of vibrating structures. The notation for describing different modes of a 3-D body is (nodal diameters, nodal circles). Figure 5 shows 6 different mode shapes of a circular disk.

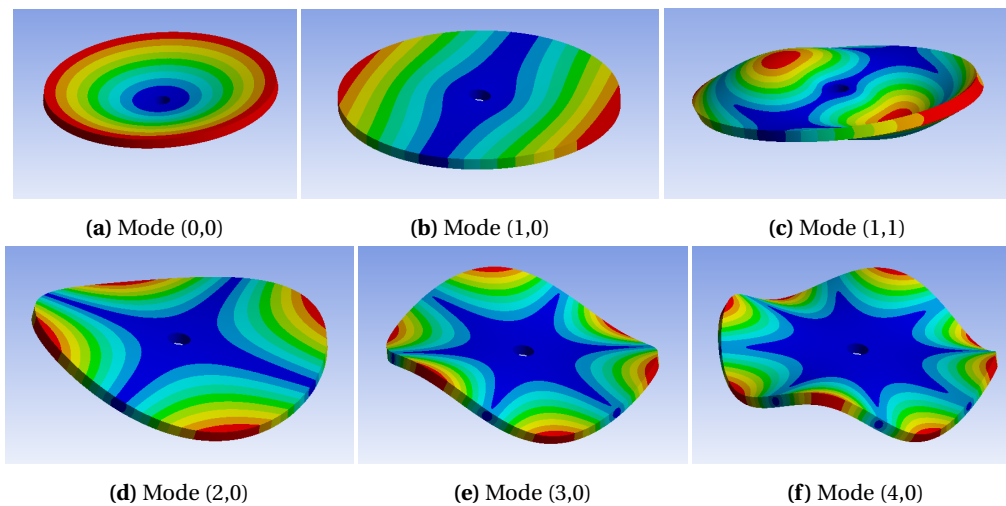


Figure 5

2.3 EXCITATION FORCES ON TURBINES

The natural frequency of a turbine is determined by the material and mass of the structure in addition to the boundary conditions. The natural frequency can be obtained by suspending the turbine in free air and hitting it with a hammer. What makes it more complicated is the fact that a turbine in operation is not suspended in free air. The turbine is connected to a generator through a shaft and confined within a small space with high water pressure and velocity. These factors severely complicates the task of precisely calculating the natural frequencies. The excitation forces on the turbine are easier to find and are caused by pressure oscillations.

2.3.1 RUNNER FREQUENCY

The runner frequency would appear if there is damage to a runner blade or if the runner or flow is unbalanced [10].

$$f_r = \frac{n_r}{60} \quad (8)$$

Where:

n_r = Runner rotational speed in RPM

f_r = Runner frequency [Hz]

2.3.2 BLADE PASSING FREQUENCY

The blade passing frequency is created each time a runner blade passes a guide vane [10].

$$f_{gv} = \frac{Z_r n_r}{60} \quad (9)$$

Where:

Z_r = number of runner blades

This frequency is usually the dominant frequency during steady state operation. The turbine produces a lot of noise when high amplitudes of this frequency occur [39]. The amplitude of the blade passing frequency is affected by the distance between the guide vanes and the runner blades.

2.3.3 GUIDE VANE FREQUENCY

The guide vane frequency is created by the runner blades passing through the guide vane wakes, see Figure 6.

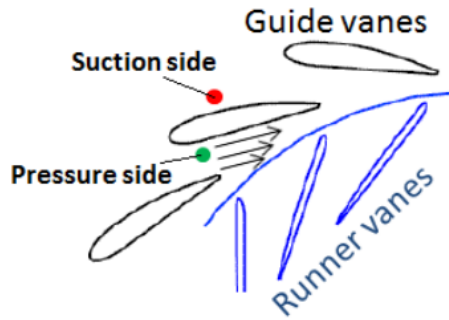


Figure 6: Wake created by the guide vanes which the runner blades hit as they rotate [39].

$$f_b = \frac{Z_{gv} n_r}{60} \quad (10)$$

Where:

Z_{gv} = number of guide vanes [Hz]

There are two essential parameters which can decrease the amplitude of this pulse. First, the distance between runner blade and guide vane. Second, the guide vane geometry [39]. This frequency is thought to be the one creating the highest pressure pulsations in Francis turbines [10, 15].

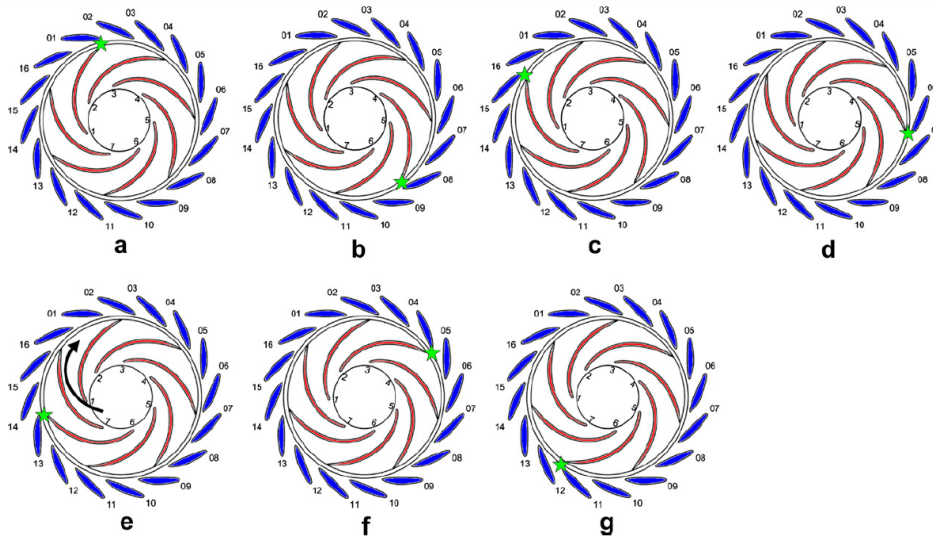


Figure 7: RSI phenomena and sequence of interaction. Runner rotating clockwise. [15]

There are also other phenomena capable of causing vibrations in and around the runner. Examples of these are vortices, vibrations caused by transient flows in the penstock, vortex ropes in the draft tube, self-excitation vibration among others. In this report the main focus will be on the RSI frequencies.

The shape of the pressure pulsations originating from the RSI shows an almost regular sine wave. Figure 7 displays a sequence from the rotation of a turbine consisting of 7 blades and 16 guide vanes. The first

interaction happens when blade 1 interacts with guide vane 1. When the runner rotates a little clockwise blade 4 meets guide vane 8, then blade 7 faces guide vane 15 and so on. Each blade receives the same pressure pulsations, but with a phase shift. The number of guide vanes and runner blades determine which mode is excited. The amplitude of the pressure pulsations depends, as mentioned above, on the head, operating conditions and design of the runner and guide vanes [15].

The shape of the pulsations generated by the RSI can be determined by the following equation [18]:

$$mz_{gv} \pm k = nz_r \quad (11)$$

Where:

m, n = integers

k = diametrical mode

The pump-turbine, which was used in this experiment, consists of 6 blades and 28 guide vanes. Using Equation 11, the main diametrical mode of excitation is $k = 2$, rotating in the same direction as the runner, or $k = 4$, rotating opposite to the runner rotation.

The frequency of which the turbine is forced to vibrate under the influence of the RSI is [18, 15]:

$$f_r = nZ_g N \quad (12)$$

Where:

N = Runner rotations per second

The pump-turbine runner in our case rotates with 10,8 rps at BEP (see Table 4). Using Equation 12 a RSI frequency of $n * 28 * 10,2 = 302,4n [Hz]$ will be generated. It means that the induced frequencies, observed from a stationary point of view will be 302,4 Hz, 604,8 Hz, 907,2 Hz and so on. To build a Francis turbine without high fatigue loads, it is important to keep the natural frequencies of the turbine away from the excitation frequencies created during operation. Therefore, as mentioned, being able to accurately determine the natural frequencies of a new runner is therefore important to ensure safe operation.

3 STRUCTURAL ANALYSIS

Structural analysis is the determination of the effects of loads on physical structures [26]. It is a way of testing materials in order to find out how much they can withstand, without doing full scale tests. It can be used to calculate the effect of wind on a bridge, a cars behaviour over a bump, the load a vein is feeling from the flowing blood inside it, the natural frequencies of a structure, etc.. To perform an accurate structural analysis, determination of the geometry of the structure, environment, loads, supports and material properties are essential. There are three approaches to solve a structural analysis. The "mechanics of materials"-approach is the simplest. It applies to simple geometries and can be solved by hand. The elastic theory-approach applies to an elastic body of any shape. Simple geometries can be solved by hand, more complex geometries must be solved with a numerical solution method [26]. The most advanced method for doing a structural analysis is with numerical approximation techniques. The basis of the analysis is the numerical approximation of the differential governing equations (equation of motion, Navier-Stokes equation, continuity equation etc.). Obtaining a solution requires computer power. The advantage of this approach, compared to the simpler methods, is its ability to handle complex geometries and boundary conditions, which often is essential. There are developed different numerical solution methods including the finite difference method, the boundary element method, the finite volume method, meshless method, the assumed-modes method and the finite element method (FEM) among others [31, 32, 37]. The basic concept of all these methods is to replace continuous models with discrete models. That means to replace the partial differential equations (PDEs) of the model and transfer them into ordinary differential equations (ODEs). Each of the methods has its pros and cons, but the most common used method is the FEM. It is also the method implemented in ANSYS software, which will be used in the simulations in this report.

3.1 FINITE ELEMENT METHOD

The birth of the FEM originates from the need to solve complex structural analysis problems in civil and aeronautical engineering [29]. The method was developed by a number of different scientists in the 1960s. The first book was published by Zienkiewicz in 1967 [32]. The concept is to divide the structure into a finite number of elements interconnected at a finite number of nodes [27]. An analogy that is used to describe this network is a "sea of springs".

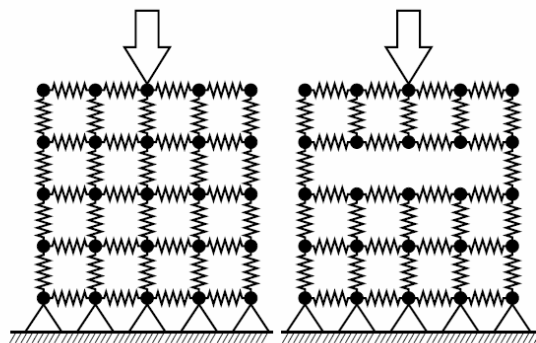


Figure 8: "Sea of springs" [32]

The springs are the edges of the elements, while the masses are the nodes within the FEM. Loads are applied at the nodes. These loads are caused by external or internal forces. Material properties decide the stiffness and damping of the springs. An applied load will put stresses on the springs and they will deflect according to their stiffness. By removing some of the springs, the geometry of the model is changed. The

deflection of the nodes and springs will also change altering the response of the structure. Dividing the structure into smaller elements increases the accuracy of the calculations.

All engineering phenomena can be expressed by governing equations and boundary conditions. The FEM approximates the equations and boundary conditions to a set of algebraic equations which can be solved numerically. These equations dictate the physical behavior inside the elements. The Navier-Stokes equations, continuity equation, Newton's second law or momentum equation is used based on the problem to solve. These sets of equations are then solved, one element at a time [33]. For models of useful size, the number of equations and unknowns are large and solving them by hand is not an option. Fortunately, computers are excellent for such jobs, but the governing equations need to be discretized in order to be solved. The general pattern for these algebraic equations are [32]:

$$[Property]\{Behavior\} = \{Action\} \quad (13)$$

In case of the simple spring system in Figure 9b, the property is the stiffness of the spring, the behaviour is the displacement and the action is the load applied to the spring.

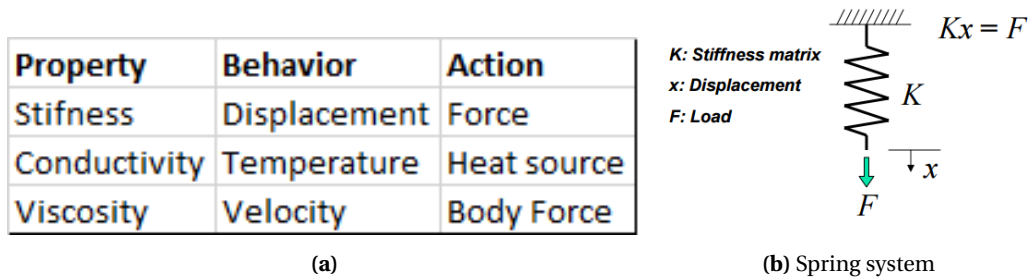


Figure 9

As mentioned above, the big advantage of the FEM, and the main reason why it is the most commonly used method of structural analysis today, is its ability to handle complex geometries and loading situations [32]. This is an important attribute in many engineering applications.

3.2 FEM IN ANSYS

The general equation of motion for a structural system, used in ANSYS, is given as [28]:

$$[M]\{\ddot{u}(t)\} + [C]\{\dot{u}(t)\} + [K]\{u(t)\} = \{F(t)\} \quad (14)$$

Where:

- [M] = Structural mass matrix
- [C] = Structural damping matrix
- [K] = Structural stiffness matrix
- $\{\ddot{u}(t)\}$ = Nodal acceleration vector
- $\{\dot{u}(t)\}$ = Nodal velocity vector
- $\{u(t)\}$ = Nodal displacement vector
- $\{F(t)\}$ = Applied load vector

Compared to Equation 13, the [M], [C] and [K] matrices are the property of the system, $\{u\}$ is the behaviour and $\{F(t)\}$ is the action.

As mentioned, solving a FEM can be extremely computer demanding. Based on the complexity of the simulations, some of the parameters in Equation 14 are often omitted because they are zero or so small that they do not impact the solution. ANSYS has developed different modules, specialised for solving various problems. In the field of acoustic and vibration investigation, several different modules are available. For frequency analysis, which will be performed in this report, the Modal and Harmonic response analysis will be used. Because of limitations of computer power the Transient analysis module, which is more complex and gives more possibilities for user customization, will not be used.

The [C]-matrix contains the damping coefficients. In natural frequency simulations of structures in air, the damping values are believed to be neglectable [11]. Submerged in water the damping ratio increases, but the values are still small. When the submerged structure is placed close to a solid wall, the effect of damping increases further. Valentin (2014) [11] reported that walls close to a submerged turbine doubled the Frequency Reduction Ratio (FRR) compared to a situation without any surrounding walls [11]. In these cases, being able to accurately calculate the damping effects, gets important. In the simulations performed in this report, without any near-by walls, the exclusion of damping should not impact the results that much. On real operating turbines however, where distances to solid walls are small, damping effects are important and should be accounted for when doing simulations. In this report the modal analysis simulations are calculated without damping effects, while in the harmonic response analysis, damping effects are included.

3.2.1 MODAL ANALYSIS

Modal Analysis is used to calculate natural frequencies and mode shapes of structures. The module is subjected to certain restrictions. These are constant stiffness and mass effects, no damping effects and no time varying forces or other loads [28]. Under these restrictions Equation 14 can be simplified:

$$[M]\{\ddot{u}\} + [K]\{u\} = 0 \quad (15)$$

The free vibrations of the structure will be harmonic [27, 28]:

$$\{u\} = \{\phi\}_i \cos(\omega_i t) \quad (16)$$

Where:

$\{\phi\}_i$ = eigenvector representing the mode shape of the i th natural frequency

$\omega_i t$ = i th natural circular frequency

t = time

Substituting Equation 16 into Equation 15 gives:

$$(-\omega_i^2[M] + [K])\{\phi_i\} = 0 \quad (17)$$

The trivial solution is $\{\phi_i\} = 0$, while the solution of interest looks like this:

$$|[K] - \omega^2[M]| = 0 \quad (18)$$

This is a standard eigenvalue problem and is solved to find the natural frequencies (eigenvalues) ω_n and the mode shapes (eigenvectors) $\{\phi_n\}$ of the system. In Modal analysis solver control option, there are 4 choices for how to solve this eigenvalue problem.

3.2.1.1 Direct solver

In the direct solver option Block Lanczos method is used to extract the eigenvalues at each iteration. Without being too detailed, this method is a specialised form of the classical Lanczos algorithm. The Lanczos recursions are performed using a block of vectors, as opposed to a single vector, which is the basis of the classical Lanczos algorithm [28]. As described in Section 3.1 and by Equation 13 the problem to solve consists of a set of matrices:

$$[K]\{u\} = [F] \quad (19)$$

The different solver options represent different methods for solving these sets of equations. The direct method is primarily a Gaussian elimination process and direct elimination of the equations. The $[K]$ matrix is decomposed into lower and upper triangular matrices, $[K] = [L][U]$. Then forward and back substitutions using $[L]$ and $[U]$ are made to compute the solution vector $\{u\}$ [28]. The direct solver in ANSYS uses the fact that the finite element matrices often are sparsely populated to minimize the number of equations that need to be solved. Because of the direct procedure, the method has large disk and memory requirements [24].

3.2.1.2 Iterative solver

An iterative solver is based on an initial guess, which through an iterative process is refined until the solution is within a pre set tolerance value. When choosing the iterative solver, ANSYS will use the PCG (Preconditioned Conjugate Gradient) Lanczos method to extract the eigenvalues. The basis of the extraction procedures is the same as for the Block Lanczos method but there are some small differences, which among others, makes PCG Lanczos only available in modal calculations. At every iteration step an iterative solution procedure is used. The advantage of the iterative solution compared to the direct solver is that it normally will be faster as each step is less computer demanding. On the other hand, convergence is not guaranteed and an iterative solver is less robust and may need many iterations to reach a solution [24].

3.2.1.3 Unsymmetric solver

The unsymmetric eigensolver is used when the system of matrices are unsymmetric, which is the case in Fluid Structure Interaction (FSI) problems. The solver uses a method capable of handling the unsymmetric matrices which arises in models containig FSI boundaries. The method is called Frequency Derivative Method and uses an orthogonal set of sequence vectors to get rid of the unsymmetric matrices. The solver process is done by a direct solver method. A transformation equation is applied to obtain the converged eigenvectors [28]. An unsymmetric solver generally has longer solution times and requires more computer power than the direct solver.

3.2.1.4 Supernode solver

The Supernode method is used to solve large, symmetric eigenvalue problems for many modes (up to 10000 and beyond). The solver uses methods comparable to the Block Lanczos and PCG Lanczos, but is faster if the requested number of modes is in excess of 200 [28]. In this report the number of requested modes will not be so high that the supernode solver will be used.

3.2.2 HARMONIC RESPONSE ANALYSIS

The other module from the ANSYS Mechanical workbench which will be used in this report is the Harmonic response analysis. The main difference between the harmonic response analysis and the modal analysis module is the possibility of applying harmonically time-varying loads to the structure. As the exciting forces from the RSI also varies harmonically [19, 15], the simulations offer the possibility of applying pressure forces on the runner similar to what it would experience in operation. All applied loads vary sinusoidally. Unlike modal analysis, harmonic response analysis take the effect of damping into account. Based on these restrictions, Equation 14 can be written:

$$[M]\{\ddot{u}\} + [C]\{\dot{u}\} + [K]\{u\} = \{F^a\} \quad (20)$$

Where:

F^a = applied load vector, varies sinusoidally.

All the points in the structure are moving at the same frequency, but not necessarily in phase. Therefore the displacement may be defined as [28]:

$$\{u\} = \{u_{max}e^{i\phi}\}e^{i\Omega t} \quad (21)$$

Where:

u_{max} = maximum displacement

Ω = imposed circular frequency (radians/time)

ϕ = displacement phase shift (radians)

This equation can be rewritten as [28]:

$$\{u\} = (\{u_r\} + i\{u_{img}\})e^{i\Omega t} \quad (22)$$

Where:

u_r = real displacement vector

u_{img} = imaginary displacement vector

In the same manner, the force vector is specified [28]:

$$\{F\} = (\{F_r\} + i\{F_{img}\})e^{i\Omega t} \quad (23)$$

Where:

F_r = real force vector

F_{img} = imaginary force vector

Substituting Equation 22 and Equation 23 into Equation 20 gives:

$$(-\Omega^2[M] + i\Omega[C] + [K])(\{u_r\} + i\{u_{img}\})e^{i\Omega t} = (\{F_r\} + i\{F_{img}\})e^{i\Omega t} \quad (24)$$

Time dependency is the same on both sides and can be removed, leaving:

$$([K] - \Omega^2[M] + i\Omega[C])\{u_r\} + i\{u_{img}\} = \{F_r\} + i\{F_{img}\} \quad (25)$$

Equation 25 is expressed in the form of Equation 13 and then solved directly using primarily a Gaussian elimination approach [28]. The possibility of time varying forces in the harmonic response analysis makes it possible to plot the results in form of a Bode plot. As opposed to the modal analysis, where the results only contains the natural frequencies of the different modes, the harmonic response gives the structural deformations for the whole range of frequencies.

3.2.2.1 Solution method

In Harmonic response analysis there are two different options. The Full analysis and the Mode-Superposition analysis. The difference between the two methods is the treatment of the damping ratios. In the full analysis option the damping matrix is calculated explicitly in the model using this expression for [C] [28]:

$$[C] = \alpha[M] + (\beta + \frac{1}{\Omega}g)[K] + \sum_{i=1}^{N_{ma}} \alpha_i^m [M_i] + \sum_{j=1}^{N_m} [(\beta_j^m + \frac{2}{\Omega}m_j + \frac{1}{\Omega}g_j^E)[K_j]] + \sum_{k=1}^{N_e} [C_k] + \sum_{m=1}^{N_v} \frac{1}{\Omega} [K_m] + \sum_{l=1}^{N_g} [G_l] + \frac{1}{\Omega} \sum_{k=1}^{N_e^*} [K_k^*] \quad (26)$$

Where:

α = mass matrix multiplier, β = stiffness matrix multiplier, g = constant structural damping coefficient, N_{ma} = number of materials, α_i^m = stiffness matrix multiplier for material i, M_i = portion of structural mass matrix based on material i, N_m = number of materials with damping input, β_j^m = Stiffness matrix multiplier for material j, m_j = constant structural damping coefficient for material j, g_j^E = structural damping coefficient for material j, $[K_j]$ = portion of structural stiffness matrix based on material j, N_e = number of elements with specified damping, $[C_k]$ = element damping matrix, N_v = number of elements with viscoelastic damping, $[K_m]$ = element viscoelastic damping matrix, N_g = number of elements with Coriolis or gyroscopic damping, $[G_l]$ = element Coriolis or gyroscopic damping matrix, N_e^* = number of elements with specified imaginary stiffness matrix, $[K_k^*]$ = imaginary element stiffness matrix

Substituting this into Equation 25 yields the harmonic response equation of motion, which is solved in the simulation, when the full analysis option is used. When using the Mode-superposition analysis the damping matrix is not explicitly computed, but rather defined directly in terms of a damping ratio [28]:

$$\zeta_i^d = \zeta + \zeta_i^m + \frac{\alpha}{2\omega_i} + \frac{\beta}{2}\omega_i \quad (27)$$

Where:

ζ = constant modal damping ratio, ζ_i^m = modal damping ratio for mode shape i, ω_i = circular natural frequency associated with mode shape i = $2\pi f_i$, f_i = natural frequency associated with mode shape i

In the simulations in this report the Full analysis solution is applied.

4 STRUCTURAL ACOUSTICS

Structural acoustics are the study of the mechanical waves in structures and how they interact with and radiate into adjacent media [30]. That translate, for the purpose in this report, to the interaction between vibrations in fluids and solids.

A fluid has the ability to greatly effect the frequencies of a submerged structure [2, 3, 4, 19, 8]. When a submerged structure vibrates, energy is dissipated to the surrounding fluid. It means that some of the energy in the vibrations of the structure is being consumed by setting the surrounding fluid in motion. Based on the density and viscosity of the fluid, the vibrations are reduced compared to the structure vibrating in vacuum. If the fluid has a high viscosity and density, thus needing more energy to be set in motion, more energy is dissipated in comparison to a less dense or less viscous fluid. The effect can be viewed as adding mass to the vibrating structure and consequently lowering its natural frequency. The reduced natural frequency observed is called the added mass effect. Air is a medium with low density and viscosity compared to metal and the added mass effect is negligible. Water however, has a much higher density and viscosity and has a large effect on the natural frequencies of structures submerged in it. To be able to accurately calculate the phenomena, the added mass effect must be accounted for. A measure of how much the frequency is reduced is given by the Frequency Reduction Ratio (FRR) [13]:

$$\delta = \frac{f_{air} - f_{water}}{f_{air}} \quad (28)$$

The FRR caused by the added mass effect has been reported to be as high as 0,8 for turbine runners [20], but this number is highly dependent on the the shape and properties of the submerged material.

4.1 FLUID SOLID INTERACTION

Numerical simulations of structures in fluid environments are called Fluid-Structure Interaction (FSI) simulations. To be able to solve them correctly, the influence of the fluid must be taken into account and the governing equation for fluid motion must be utilized. To model the behavior of the fluid, the Navier-Stokes and continuity equations is considered. These equations are extensive and detailed. To make the simulations more manageable some assumptions are being made. The fluid is slightly compressible, where density changes are due to pressure variations and there is no mean flow of the fluid [28]. The Navier-Stokes equation and the continuity equation can then be simplified, giving the acoustic wave equation [28]:

$$\nabla\left(\frac{1}{\rho_0}\nabla p\right) - \frac{1}{\rho_0 c^2}\frac{\partial^2 p}{\partial t^2} + \nabla\left[\frac{4\mu}{3\rho_0}\nabla\left(\frac{1}{\rho_0 c^2}\frac{\partial p}{\partial t}\right)\right] = -\frac{\partial}{\partial t}\left(\frac{Q}{\rho_0}\right) + \nabla\left[\frac{4\mu}{3\rho_0}\nabla\left(\frac{Q}{\rho_0}\right)\right] \quad (29)$$

Where:

c = speed of sound in fluid

ρ = mean fluid density

μ = dynamic viscosity

p = acoustic pressure

Q = mass source in the continuity equation

t = time

This differential equation describes the motion of the fluid that surrounds the structure. As mentioned in Section 3.1, the equation needs to be discretized to make it usable for numerical calculations. After some manipulation and by using the Galerkin procedure [28], the discretized wave equation is obtained [28]:

$$[M_F]\{\ddot{p}_e\} + [C_F]\{\dot{p}_e\} + [K_F]\{p_e\} + \bar{\rho}_0[R]^T\{\ddot{u}_e\} = \{f_F\} \quad (30)$$

Where:

$[M_F]$ = acoustic fluid mass matrix
 $[C_F]$ = acoustic fluid damping matrix
 $[K_F]$ = acoustic fluid stiffness matrix
 $[R]^T$ = acoustic fluid boundary matrix
 $\{f_F\}$ = acoustic fluid load vector
 $\bar{\rho}_0$ = acoustic fluid mass density constant
 p_e = nodal pressure vector
 u_e = nodal displacement vector

This equation handles the fluid part of the model. To complete the system, we need a part in the equation of motion for the structural system able to handle the boundary between the solid and fluid domain. The coupling conditions on the interface can be expressed as [28]:

$$\bar{\sigma}(\vec{u}_S)\vec{n} + p\vec{n} = 0 \quad \text{on } FS \quad (31)$$

$$\vec{n} \cdot \vec{u}_S - \vec{n} \cdot \vec{u}_F = 0 \quad \text{on } FS \quad (32)$$

Where:

$\bar{\sigma}(\vec{u}_S)$ = solid stress tensor
 \vec{u}_S = displacement in acoustic fluid
 \vec{u}_F = displacement in acoustic fluid
 \vec{n} = outward normal unit vector of fluid domain
 FS = fluid-solid boundary

The combination of equation of motion for the structural (Equation 20) and fluid (Equation 30) parts of the system and applying the boundary coupling conditions on the interface (Equations 31 and 32) give:

$$\begin{bmatrix} [M_S] & [0] \\ [\bar{\rho}_0[R]^T & [M_F] \end{bmatrix} \begin{Bmatrix} \{\ddot{u}\} \\ \{\ddot{p}\} \end{Bmatrix} + \begin{bmatrix} [C_S] & [0] \\ [0] & [C_F] \end{bmatrix} \begin{Bmatrix} \{\dot{u}\} \\ \{\dot{p}\} \end{Bmatrix} + \begin{bmatrix} [K_S] & -[R] \\ [0] & [K_F] \end{bmatrix} \begin{Bmatrix} \{u\} \\ \{p\} \end{Bmatrix} = \begin{Bmatrix} \{f_S\} \\ \{f_F\} \end{Bmatrix} \quad (33)$$

Which is solved to give the natural frequencies. As mentioned in Section 3.2.1.3, unsymmetric matrix systems requires more computer resources to solve. By introducing the transformation $\dot{u} = j\omega$ the displacement and pressure differentials are removed in the system of Equation 33 and we obtain this discretized equation [27]:

$$\begin{bmatrix} -\omega^2[M_S] + j\omega[C_S] + [K_S] & -[R] \\ -\omega^2\bar{\rho}_0[R]^T & -\omega^2[M_F] + j\omega[C_F] + [K_F] \end{bmatrix} \begin{Bmatrix} \{u\} \\ \{p\} \end{Bmatrix} = \begin{Bmatrix} \{f_S\} \\ \{f_F\} \end{Bmatrix} \quad (34)$$

This matrix on the left hand side is unsymmetric. Solving it for nodal pressures and displacements demands the inversion of this unsymmetrical matrix. This process needs a significant amount of computer power. For matrices having the right attributes, ANSYS offers a way of transforming the unsymmetric matrices into symmetric ones before initiating solving procedures. For the harmonic response analysis this is performed by introducing a transformation variable for the nodal pressures [27]:

$$[\dot{q}] = j\omega[q] = p \quad (35)$$

By using this transformation there is possible to transform the unsymmetric Equation 34 into a symmetric matrix [27]:

$$\begin{bmatrix} -\omega^2[M_S] + j\omega[C_S] + [K_S] & -j\omega[R] \\ -j\omega[R]^T & \frac{\omega^2[M_F]}{\bar{\rho}_0} - \frac{j\omega[C_F]}{\bar{\rho}_0} - \frac{[K_F]}{\bar{\rho}_0} \end{bmatrix} \begin{Bmatrix} \{u\} \\ \{q\} \end{Bmatrix} = \begin{Bmatrix} \{f_S\} \\ \frac{j}{\omega\bar{\rho}_0} \{f_F\} \end{Bmatrix} \quad (36)$$

Which can be solved, obtaining the nodal displacement u and the transformation variable for the nodal pressures q . The nodal pressure p can then be calculated using Equation 35. For the modal analysis module this transformation is not possible because of the involvement of frequency [22]. To solve this problem a displacement potential, Φ , is introduced. This leads to [22]:

$$\vec{u}_F = \frac{\bar{\rho}_0}{\rho_F} \nabla \phi \quad (37)$$

Introducing this transformation in the continuity and momentum equations and in the coupling conditions in Equation 31 and 32 the following lossless symmetric eigen matrix equation can be derived [22]

$$-\omega^2 \begin{bmatrix} M_S & 0 & 0 \\ 0 & 0 & 0 \\ 0 & 0 & \bar{\rho}_0 K_F \end{bmatrix} \begin{Bmatrix} \{u_e\} \\ \{p_e\} \\ \{\phi_e\} \end{Bmatrix} + \begin{bmatrix} K_S & -R & 0 \\ -R^T & -\frac{1}{\bar{\rho}_0} M_F - \frac{1}{\bar{\rho}_0} S_F & K_F \\ 0 & K_F^T & 0 \end{bmatrix} \begin{Bmatrix} \{u_e\} \\ \{p_e\} \\ \{\phi_e\} \end{Bmatrix} = 0 \quad (38)$$

This matrix system is then solved in the modal analysis module when doing FSI analysis with a symmetric solver. Even if the transformation demands extra computer power, the fact that the system now is symmetric may give time savings that exceeds the losses during transformation.

There are different FSI simulations available. In 1-way FSI the results from the fluid pressure are transferred to the solid body only when the simulations starts. After that no response from the structural movement is returned to the fluid. In 2-way FSI the results from the structural movement are transferred back to the fluid at every iteration. In the case of vibration of turbines, the displacement of the structure is small and no separation of the flow occurs at the boundary. Consequently, the influence of the structure on the water is very little. In addition, to be able to detect the high frequency vibrations of above 1000 Hz, the time steps must be very small and the computer resources needed are very high. Dompierre and Sabourin (2010) [34], using a 12 GB RAM computer on a 799900 node model of a turbine runner, used 95 days on the numerical calculations with a 2-way FSI model. The results obtained by the 2-way FSI method were more or less similar to those obtained by the 1-way FSI simulation. Zhu et al. (2012) [35] confirms this, stating that if deformation is low, which is the case for vibrating turbines, 1-way FSI produces results similar to those obtained by 2-way FSI simulations. Based on the computer power available, 1-way FSI is used in this report.

4.2 FLUID ELEMENTS

In structural acoustic simulations there are both fluid and structural elements involved. The fluid elements can be formulated in two different ways, either displacement formulated or pressure formulated. The pressure formulated elements use acoustic nodal pressure for the calculations, as in Equation 30, while displacement formulated elements are based on the physical movement of the nodes, as in the equation of motion for the structure. When using displacement formulated elements for the acoustic part of the model the underlying material behavior is altered, compared to structural elements. To reflect the behavior of a

fluid, the stiffness terms associated with shear stresses are set to near zero and the Young's modulus is set equal to the bulk modulus. This means that the element has no ability to resist shear stress [27]. There are some advantages of the displacement formulated elements. Because the elements have similar degrees of freedom as the structural elements, all the elements on the FSI can be directly coupled, without needing any coupling matrix. Without this coupling matrix the system is symmetric and thus facilitate a faster solving process. Figure 10 shows how displacement formulated elements work.

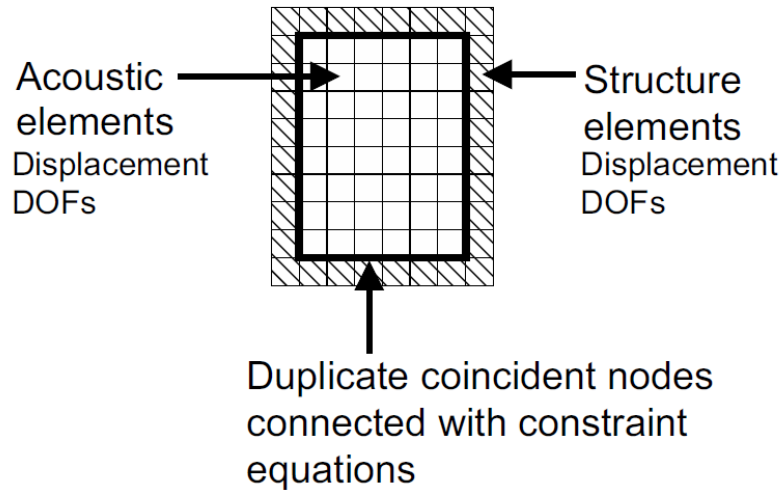


Figure 10: Displacement formulated acoustic elements [27]

When using pressure formulated elements the model will be more complex. Figure 11 illustrates the concept. The acoustic elements have only pressure degrees of freedom. The structural elements have only displacement degrees of freedom. At the interface between the acoustic fluid and the structure there is a layer of elements having both pressure and displacement degrees of freedom, which enables the coupling between vibrations in the structure and the pressure response in the fluid. To get accurate results, it is important to carefully construct the FSI [27].

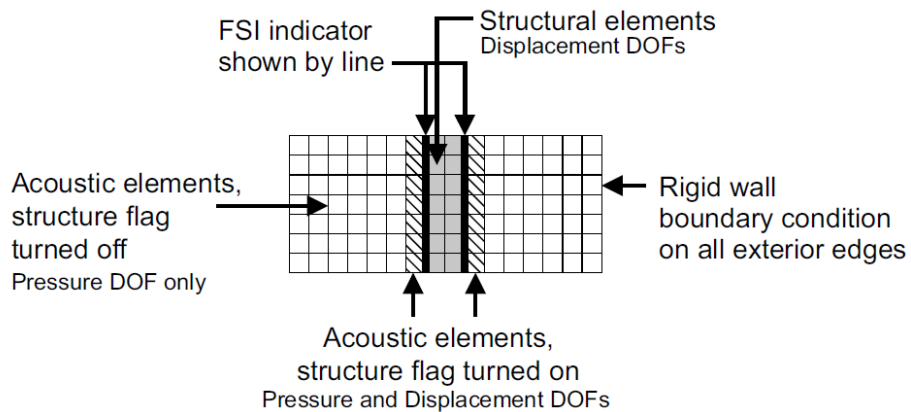


Figure 11: Pressure formulated acoustic elements [27]

Even though displacement formulated acoustic elements have its advantages, pressure formulated elements are the most used method today. The only drawback of the method is the unsymmetric set of

equations, but this problem can in many cases be resolved by using the transformation in Equation 35 or be solved with an unsymmetric solver. In ANSYS, fluid elements using displacement formulated acoustic elements are termed *legacy elements* and are not recommended to use. All simulations in this report will be performed using pressure formulated acoustic elements. As the structural elements used in the FSI simulations only have displacement degrees of freedom a transfer matrix is used to connect the structural and acoustic elements:

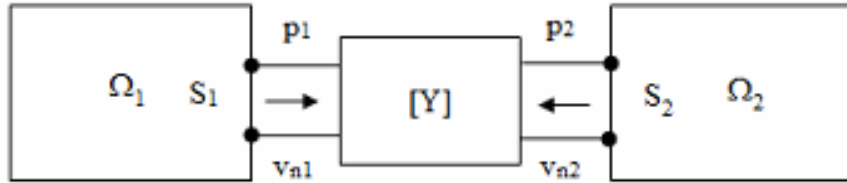


Figure 12: Visualization of the transfer matrix coupling the structural (Ω_1) and acoustic domain (Ω_2) [22]

$$\begin{Bmatrix} v_{n1} \\ v_{n2} \end{Bmatrix} = \begin{bmatrix} Y_{11} & Y_{12} \\ Y_{21} & Y_{22} \end{bmatrix} \begin{Bmatrix} p_1 \\ p_2 \end{Bmatrix} \quad (39)$$

Where:

p_1, p_2 = pressure at part 1 and 2

v_{n1}, v_{n2} = normal velocity at port 1 and 2

Y_{11}, Y_{22} = self-admittance

Y_{12}, Y_{21} = mutual admittance

5 PREVIOUS WORK DONE ON NUMERICAL SIMULATIONS OF SUBMERGED STRUCTURES

The problem of failure of turbine runners is not a new concern and much work has been put down trying to understand why these breakdowns happen. In this section some of the work that has been done on numerical simulations of turbines and FSI coupling is presented. Liang et al. (2007) [3] performed a numerical simulation to analyse the influence of the surrounding water on a turbine runner. The simulations were linked to experiments performed in Rodriguez et al. (2006) [2]. The results from the simulations were similar to those obtained in the experiment. All deviations remained within a range of $\pm 3,5$ %. The FRR was in the range of 0,10-0,39 depending on the mode shape of the structure. Lais et al. (2009) [19] did numerical and experimental tests on three different turbines. Both modal analysis and harmonic response analysis were performed. For the harmonic response analysis a CFD simulation were performed upfront to determine the pressure distribution on the blades. The numerical results showed accordance with the experimental results (± 5 %). The report concludes that even if the numerical results of the turbine submerged in water were close to the experimental results, they were not tested with any nearby structures which could significantly alter the natural frequency of the turbine. Egusquiza et al (2009) [20] did both numerical and experimental investigations on a prototype impeller. Using FEM, there were found accordance between the experiment and the numerical simulations. A FRR of 0,5-0,8 were found. Flores et al. (2012) [13] did perform both experiments and numerical simulations on a 38,5 MW Francis runner. The report finds good agreement between the experiments and the simulations, a difference of $\pm 3,5$ % between numerical and experimental results are found. A frequency reduction ratio of 0,152-0,324 was observed. In Hübner et al. (2010) [8] an investigation into the application of fluid-structure coupling was performed. Further, structural simulations comparing the impact of flowing water to still water revealed that simulations with stagnant water usually are sufficient and give good results as long as damping effects is low. Rodriguez et al. (2012) [4] tested the capability of a structural-acoustic FSI model to predict the natural frequencies of submerged structures with nearby rigid surfaces. The simulations were performed on cantilever plates. The findings suggested that the natural frequency of a submerged plate is significantly impacted by a nearby solid wall. It also showed that structural-acoustic coupling of the numerical simulations was able to predict the reduced natural frequencies of the plates. Valentin et al (2014) [17] investigated the dynamic response of a circular disk in a confined space. The results showed that the numerical simulations could predict the natural frequencies of the disk both in water and in air. The report also concludes that radial confinement has a significant impact on the vibrations of the disk and that the numerical simulations were able to detect this. The error of the numerical simulations were no more than ± 6 %. Presas et al (2014) [16] did experimental analysis on the natural frequencies of a rotating disk spinning at 8 Hz. The results showed that the natural frequency of the disk was altered by only a very small margin.

Even though most of the research on fatigue damage on turbine runners have been concerning the investigation of the natural frequencies of the turbine and the possible resonance that can arise, as mentioned in Section 2.3, there are other sources of vibration in the system. Brekke (2010) [1] is claiming that the breakdowns are not caused by resonance between the natural frequency and the RSI, but instead by sound waves caused by the pressure shock originating from the runner blades passing the guide vane wakes. These waves are propagating through the system and reflects, causing vibration and noise. This underlines the fact that the dynamics of what happens in a turbine during operation and what is causing the vibrations that leads to failure, is not fully understood.

6 NUMERICAL SIMULATIONS

The numerical simulations were carried out on a computer with Intel Core i7-2600 processor and 16 GB RAM. ANSYS Mechanical software with Acoustic ACT (Application Customization Toolkit) Extension was used, which enabled acoustic features to be accessible by GUI. A CAD model of the pump-turbine runner, made during construction of the turbine, was used in the simulations, see Figure 15. The CAD geometry had earlier been used in fluid flow analysis, therefore modifications had to be done in order to get it ready for mechanical analysis. This work consisted of cleaning the structure of unnecessary details, seal small holes between faces and repair other inaccuracies. To enable the simulation of a submerged turbine, a cylindrical-shaped enclosure was created surrounding the structure. The size of the enclosure was chosen to avoid any wall effects, which can strongly influence the natural frequencies. Prior to the simulations a mesh was created. As the computer resources are limited, the density of the mesh was chosen to give the best possible balance between accuracy and time consumption. The pump-turbine was made up of 573301 tetrahedral elements of type *SOLID187*. This is a 10-node tetrahedral element with three displacement degrees of freedom and quadratic displacement behavior [28], see Figure 13. The fluid domain is meshed with 340006 tetrahedral elements of type *FLUID221*. This is also a 10-node tetrahedral element with one pressure degree of freedom and quadratic pressure behavior between nodes. At the defined FSI, a layer of *Acoustic FSI Interface 180* elements were created with both displacement and structural degrees of freedom, coupling the structural and fluid parts [23]. Because of limited computer resources, the mesh used in the simulations was made as fine as possible without making simulation time consumption to high. A fixed support simulating an attached shaft, was used. The pump-turbine runner is a model that is used for tests at the Water Power Laboratory at NTNU. It is made of bronze with a density of 7640 kg/m^3 (see Table 1) and has six blades. The speed of sound in water was set to 1447 m/s , which is the speed of sound at 10°C . The simulations in air was conducted in vacuum. Air is less dense than bronze and will not impact the vibrations of the turbine compared to vacuum. In the results section, "air" will be used instead of "vacuum". The mode shapes compared in the result chapter is (1,0), (0,0), (2,0), (3,0), (1,1) and (4,0) (see visualization of the modes in Figure 5). The transverse modes, those without any nodal radius, are the ones thought to have the highest risk of experience resonance with the RSI. By using the Equation 11, developed by Tanaka (1990) [18], the modes that are most likely to be excited by the RSI from this particular pump turbine runner (6 blades, 28 guide vanes), is mode (2,0) and (4,0).

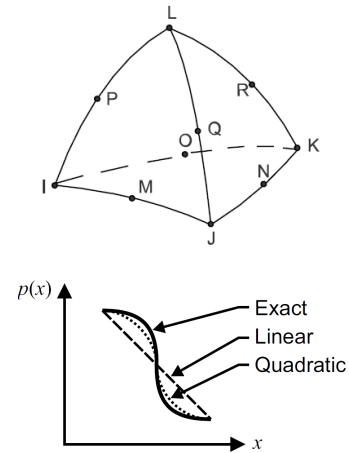


Figure 13: Above: 10-node tetrahedral element used in the simulations [28]. Below: Quadratic displacement behavior between nodes [27]

Properties	Value
Young's modulus	110 GPa
Density	7640 kg/m ³
Poisson's ratio	0,34

Table 1: Material properties of the bronze pump-turbine

	Structure	Fluid
Element type	SOLID187	FLUID221
Type of mesh	Tetrahedral	Tetrahedral
Degrees of freedom	3	1 (4 at FSI)
Number of elements	573301	340006
Number of nodes	370173	303202

Table 2: Mesh info

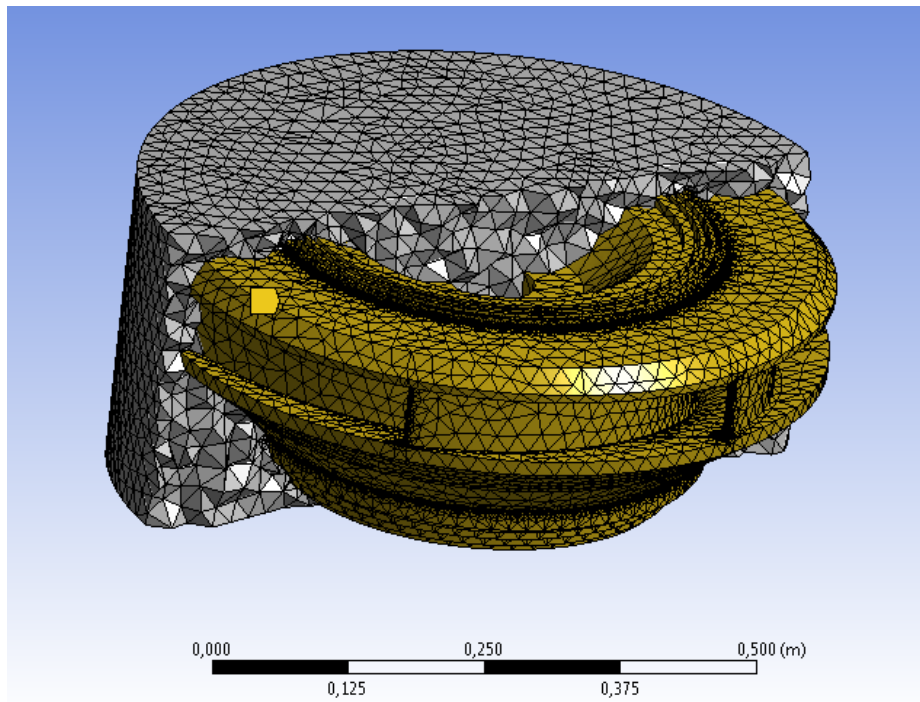


Figure 14: Visualization of the turbine and the surrounding fluid

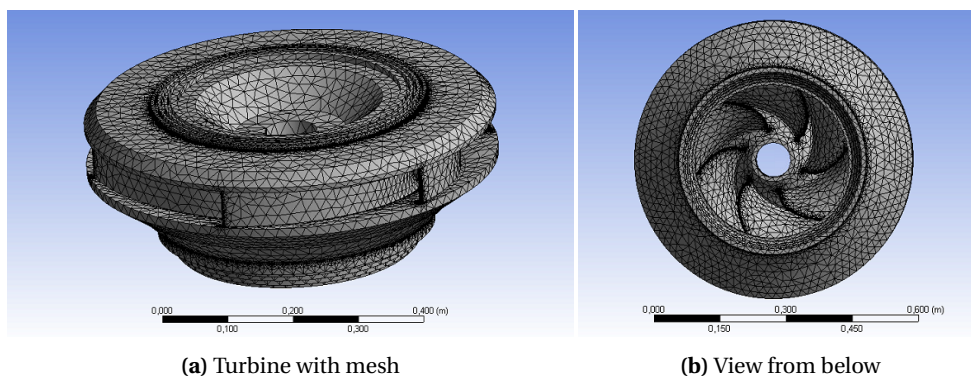


Figure 15

In the modal analysis the direct solver with Block Lanczos method was used for the extraction of the eigenvalues, see Section 3.2.1.1. The matrices solved were symmetric, using the displacement potential transformation of Equation 37 for modal analysis and the transformation of nodal pressures, Equation 35, for the harmonic response analysis. Damping effects are neglected in modal analysis. This should not have influence on the results, because damping ratios are low for these kind of simulations [19]. The full solution method was used in the harmonic response analysis, calculating the damping matrix explicitly (see Section 3.2.2.1). As mentioned in Section 3.2.2 the RSI induces a nearly sinusoidally force on the turbine. In harmonic analysis, a sinusoidally varying pressure forces with different phase angles for each blade are defined to emulate the forces put on a real turbine. The force is placed on the pressure side of each blade and a frequency sweep from 0 to 2300 Hz is performed. This frequency range was chosen to encapsulate all the frequencies observed in the modal analysis simulations. To simplify the calculations, the blade loading was assumed constant along the blade. The structural response of the pump-turbine is plotted against the frequency of the force in Figure 18.

The simulations were performed in still water and without any rotation to replicate the experiment executed by Frode Kristoffer Amundsen Kjøsnes in the Water Power Laboratory at NTNU. A fixed support was defined at the surface normally in contact with the shaft. This locks the displacement of the nodes on this surface and replicates the impact a shaft would have on the structure. In the experiment the runner is hanging from a rope and is not attached to a shaft. Valentin (2014) [11] investigated the difference between the natural frequency of a runner hung from a rope and a runner attached to a shaft. Deviations of less than 2 % for all transversal modes, except (1,0), were found. (1,0), (0,0) and (1,1) was highly dependent on the presence of the shaft. The difference in setup should, for most modes, not play an role on the results. The time consumption of the various simulations are listed in Table 3.

Simulation in air		Simulation in water	
<i>Modal</i>	<i>Harmonic</i>	<i>Modal</i>	<i>Harmonic</i>
51min	10h32min	5h50min	35h45min

Table 3: Time consumption of the simulations

Inlet diameter	0,631 [m]	n*	10,8 [1/s]
Outlet diameter	0,349 [m]	Q*	0,275[m ³ /s]
Inlet height	0,059 [m]	H*	29,3 [m]

Table 4: Pump-turbine specifications in turbine mode [38], * = at BEP

7 RESULTS AND DISCUSSION

In this section the results from the numerical simulations are presented.

7.1 MODAL ANALYSIS

The results from the modal analysis are shown in Table 5. The frequencies in air are found between 260 and 2257 Hz. The frequencies in water are found between 208-1825 Hz. A FRR between 14-34 %, depending on the mode-shape, is observed. The results are consistent with results obtained in other reports.

Mode	Air	Water	FRR
(1,0)	260	208	20 %
(0,0)	543	361	34 %
(2,0)	852	732	14 %
(3,0)	1566	1297	17 %
(1,1)	1900	1605	16 %
(4,0)	2257	1825	19 %

Table 5: Results from the modal analysis, all frequencies in *Hz*

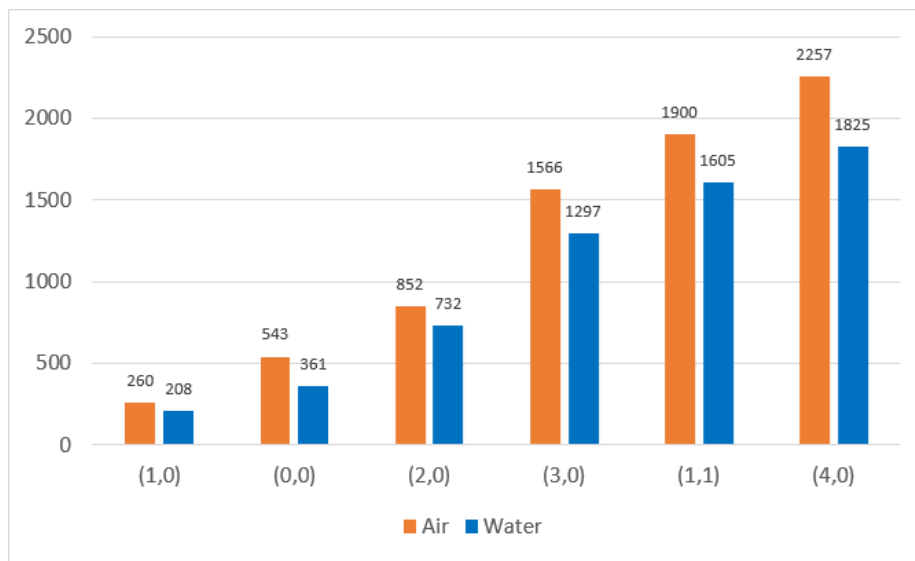


Figure 16: Comparison of frequencies in air and in water, all numbers in *Hz*

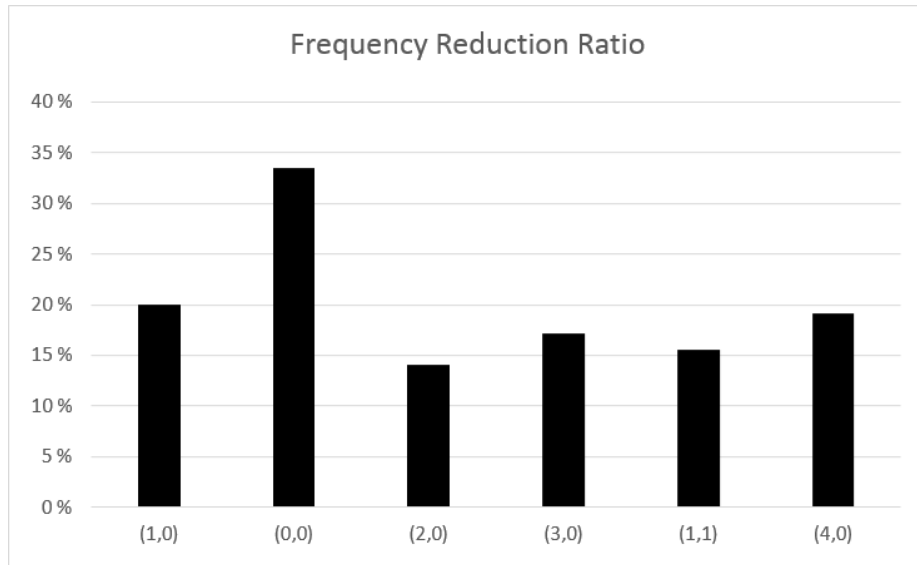


Figure 17: FRR

From the results, the added mass effect is clearly affecting the vibrations. When the turbine is submerged in water, the observed frequencies are significantly lower than the vibrations of the turbine in air. From Figure 17 variations in the reduction ratio between the different modes can be observed. The four transverse modes seem to have about the same FRR. (0,0) seems to be impacted to a higher degree by the water. Egusquiza (2009) [20] states that the highest added mass effect is observed in the modes with a relative motion between crown and band. This relative motion is not present in any of these modes. The high FRR could also mean that the displacement is higher for this mode. More movement means that more energy is dissipated to the water compared to modes with smaller displacement.

7.2 HARMONIC RESPONSE ANALYSIS

The frequency response from the harmonic response analysis is presented in Figure 18. The structural deformation is plotted against the frequency of the applied force.

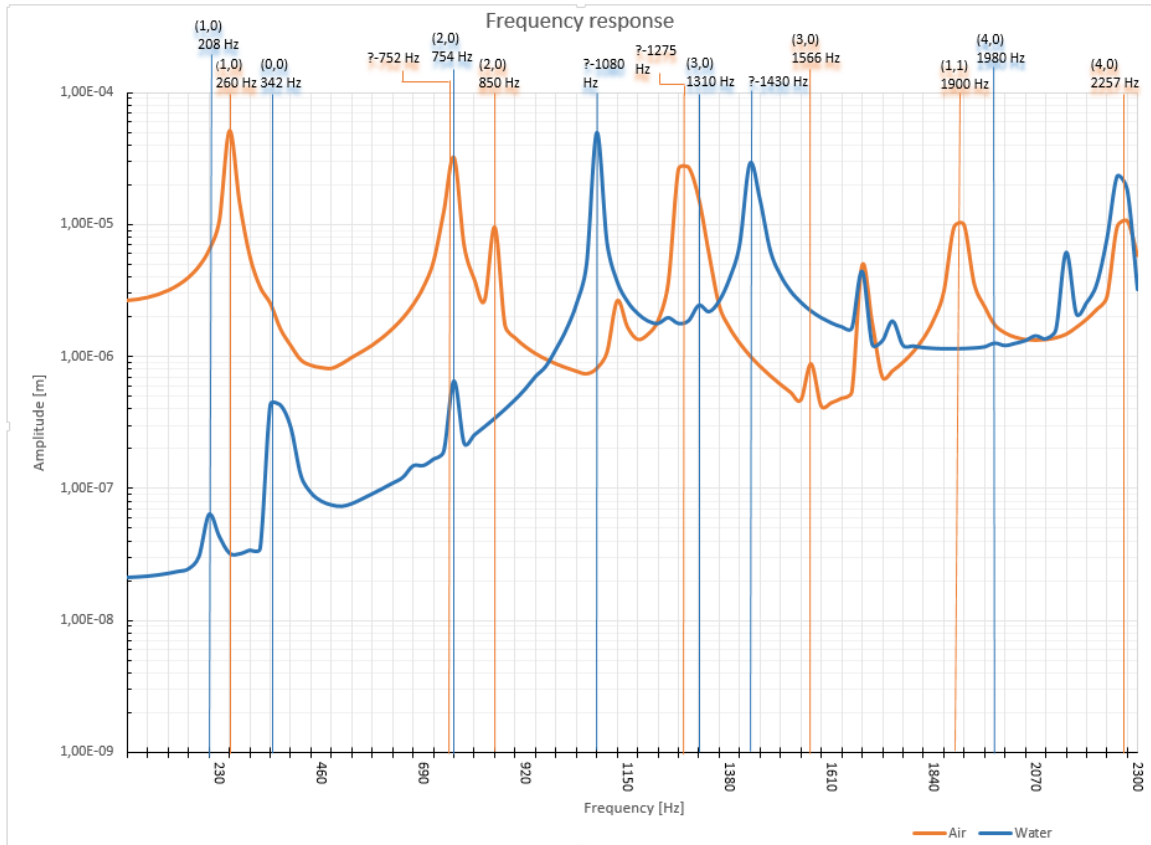


Figure 18: Comparison of the frequency response in air and in water

(1,0) is found at 208 Hz in water and 260 Hz in air. These are the same for both modal analysis (MA) and harmonic response analysis (HR) simulations. The amplitude of the deformation at 260 Hz in air is the largest of any mode inside the frequency sweep from 0 to 2300 Hz. At 342 Hz (0,0) in water is found. This frequency is more or less the same as in modal analysis. (0,0) in air is not found in the frequency response plot. The next spike is found at 752 Hz, having a shape shown in Figure 19a. This frequency has a large amplitude, but is difficult to identify. It shows signs of (1,0), but with sideways (torsion) movement. It is not too far away from the third harmonic of (1,0), which is at $(3 * 260 =) 780$ Hz. At 754 Hz (2,0) in water is found. This is a bit higher than in MA. (2,0) in air is found at 860 Hz. The higher frequency obtained for (2,0) in water leads to a lower FRR in the HR analysis compared to the MA, see Table 6. At 1080 Hz a mode in water is observed, see Figure 19b. This mode is similar to (0,0) and was not detected in MA. It has a large displacement. The mode at 1275 Hz in air is showing signs of (3,0), especially on the ring, see Figure 19c. (3,0) in water is found with a very small amplitude at 1310 Hz. This is close to the observed amplitude from the modal analysis. At 1430 Hz another unidentified mode appears. It has a similar pattern as the mode at 1080 Hz. One explanation of these two unidentified modes with similarities of (0,0), might be that they are the third and fourth harmonics of the basic (0,0) at 342 Hz. $342 * 4 = 1368$, are not that far away from 1430 Hz. The difference between the spikes is 350 Hz. The high structural deformation of these modes can possibly be related to the high frequency reduction of (0,0) in MA. When the structural displacement is high, more water is moved and more energy is dissipated when the pump-turbine is submerged in water, compared to air. At 1566 Hz, (3,0) in air is found at exactly the same frequency as in modal analysis. At 1900 Hz, (1,1) in air is found. This mode is not observed in water. (4,0) in water is found with a very small amplitude at 1980 Hz. This is a higher frequency than calculated in MA (1825 Hz). (4,0) in air is found at the same frequency as in MA. The FRR for (4,0) is consequently reduced from 19 to 12 %. Besides the four frequencies marked

in Figure 18 without any clear modes, several other spikes are also present in the frequency plot. They can be harmonics, other unidentified modes or errors from the numerical simulations.

To summarize the findings HR and MA seems to match very well in air. The simulations coincide for all modes, except that (0,0) is missing. In water the observed natural frequencies are generally a little bit higher than in MA, which are not expected. (1,1) is not found. The results from MA showed that (0,0) had a high FRR. This could indicate a high displacement. It is strange that (0,0) is not to be found from the frequency plot in air. Why it disappears is difficult to say. It might be a possibility that the result from either MA or HR concerning (0,0) is wrong or that it is shifted towards higher frequencies, either as the unidentified modes at 1080 Hz and 1430 Hz or above 2300 Hz. The experimental results from the Water Power Laboratory, listed in Table 8, found (1,0) at 1493 Hz. It might be that this is the frequency which are found at 1430 Hz in the simulations.

In water, the frequencies from HR simulations have a tendency to be higher than in MA. Table 6 shows the frequencies and FRR for the HR simulations. Table 7 shows the deviations between MA and HR simulations. For the setup of these simulations, without any nearby walls, damping ratios should be low and not impact the natural frequencies much. Even if damping effects contributes to alter the frequencies, they should be lowered and not increased as the case in these simulations. Beside the difference in excitation method, which should not alter the natural frequency of the structure, it is difficult to find any good explanation for this behavior. Sources of error include, numerical errors, input errors, model errors or similar. A complex geometry and limited computer resources may also play a role.

Mode	Air	Water	FRR
(1,0)	260	208	20 %
(2,0)	850	754	11 %
(3,0)	1566	1310	16 %
(4,0)	2257	1980	12 %

Table 6: Frequencies of modes from the harmonic response analysis

There are several other spikes, beside the ones shown in Figure 19. They are not possible to characterize with nodal lines and symmetry. Some have similarities with symmetric modes, but are not complete or show signs of torsion, others have large blade deflections. One question is if these unsymmetric modes may get into resonance with the RSI frequencies, even if the excitation forces is symmetric. The complicated nature of the pump-turbine makes it difficult to characterize all the modes. In general, the complexity of the simulations may contribute to several of the unexpected results seen.

Mode	Modal analysis	Harmonic response	Deviation
(1,0)	208	208	0 %
(2,0)	732	754	3 %
(3,0)	1297	1310	1 %
(4,0)	1825	1980	8 %

Table 7: Deviations of frequencies between modal analysis and harmonic response in water

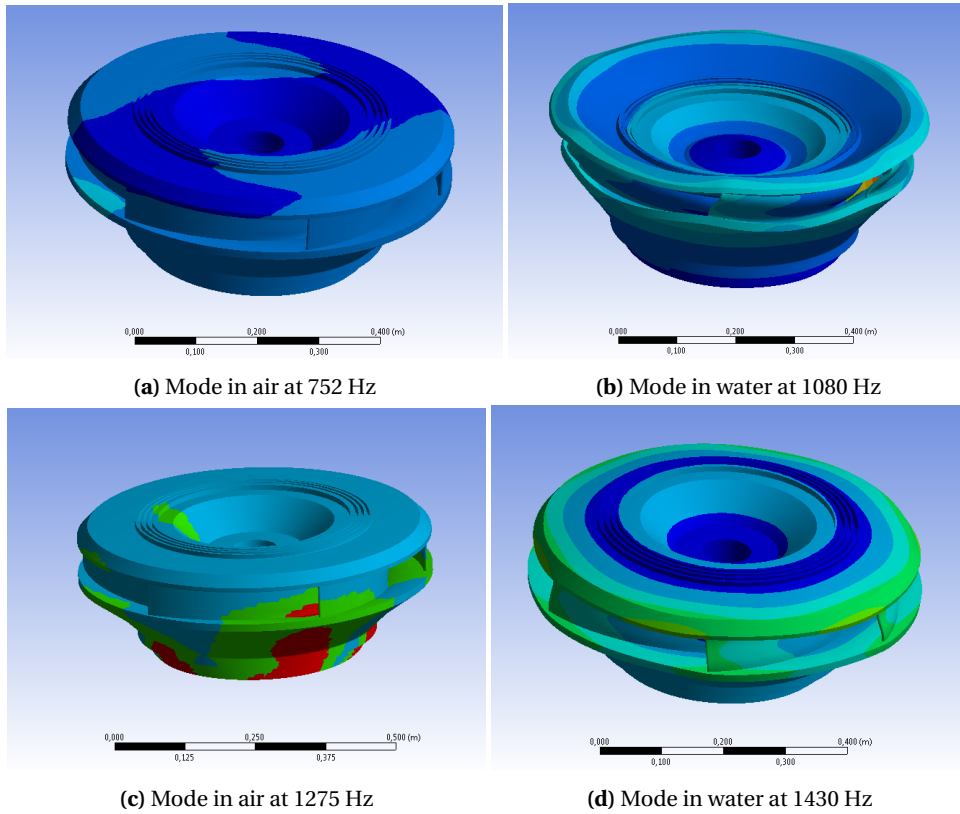


Figure 19: Deformation of modes without any clear modal patterns

7.3 EXPERIMENT

The results of the experiment at the Water Power Laboratory is shown in Table 8. The most difficult part of the experiment was to identify the different modes from the frequency response plot, see Figure 20. There are several spikes in the plot, but identifying which spike is belonging to which mode is challenging. In water they were not possible to separate.

Mode	Experiment	Simulation
(1,0)	1493	260
(2,0)	903	850
(3,0)	1110	1566

Table 8: Experimental results of the pump-turbine in air

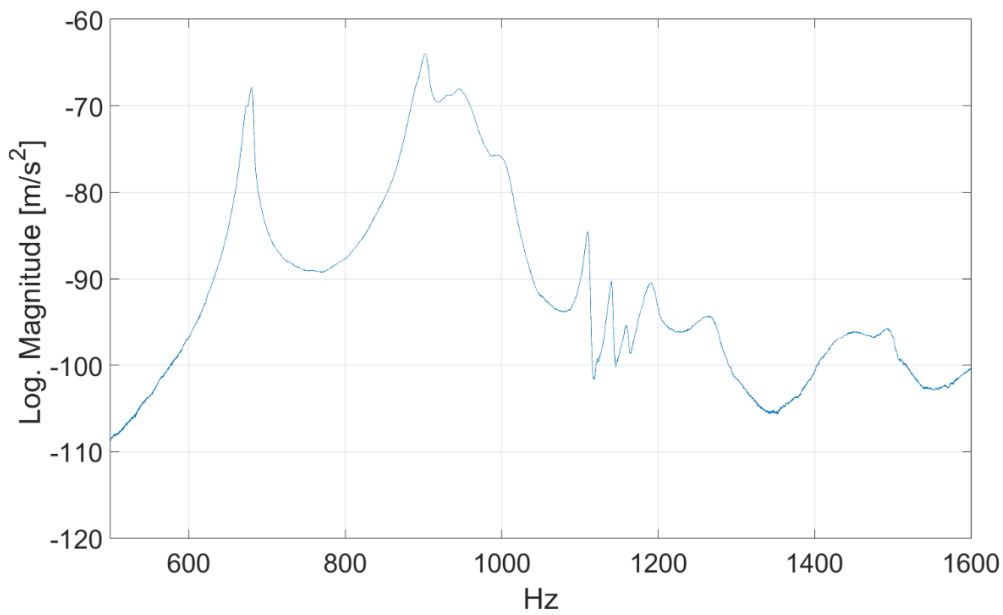


Figure 20: Frequency plot from the experiment with the pump-turbine in air

Overall, the results show poor agreement. (3,0) is far from the frequency found in the simulations. (1,0) is also far of, but this is probably not the same mode as the one observed in the numerical simulations because the difference is so big. It might be a higher harmonic of the basic mode. Or as Valentin (2014) [11] reports, (1,0) is totally dependent on the shaft. As the shaft is connected in the simulations, but not in the experiments, this might explain why the frequency for this mode does not match. (2,0) is in accordance with the numerical simulations having a deviation of only 6 %. From Equation 11, it was calculated that (2,0) and (4,0) are the frequencies which are excited by the RSI for this particular turbine. (2,0) is vibrating with much higher amplitude than (4,0) and is the main mode that may get into resonance with the RSI. The fact that the experimental and numerical results match, may indicate that the numerical simulations concerning this mode is correct.

8 CONCLUSION

In this thesis numerical simulations of a pump-turbine runner in air and in water has been performed. Using ANSYS 15 software, a CAD drawing of the pump-turbine was modified and surrounded by water to replicate an experiment performed in the Water Power Laboratory at NTNU. The goal of the simulations were to find the natural frequencies and displacements of the pump-turbine in air and in water using different simulation modules. The results of the simulations have been compared. For the simulations in water FSI coupling was used.

First, a modal analysis was performed. The results from the simulations showed a FRR of 16-34 %. The highest FRR is observed from (0,0). A harmonic response analysis were then performed. The structural deformation was plotted against the frequency. The highest displacements were found for (1,0) and (2,0) in air, and for two unidentified modes in water. The results of the harmonic response analysis in air were exactly the same as the results obtained in modal analysis simulations. The results in water showed deviations of up to 8 %. Damping is included in the calculations of the harmonic response and it is therefore strange that the observed frequencies are higher for the harmonic response analysis. Damping should increase the added mass effect thus lowering the frequencies. Simulations carried out in the Water Power Laboratory gave results that showed variable coherence. (2,0) is only off by 6 %, but both (1,0) and (3,0) is far from the simulated frequencies. The reason why (1,0) is different is probably caused by the shaft. Why (3,0) is off by such margin is more difficult to explain, but there are a number of factors in both the numerical and experimental setup that could cause this. The fact that (2,0), the mode with the highest energy content, the highest displacement and a frequency which could be excited by the RSI, is at approximately the same frequency for both experimental and numerical results indicates that this might be correct.

At BEP, the induced frequency of the RSI is $302,4 * 3 = 907,2$ Hz, which are some way of (2,0)'s natural frequency in water at 732 Hz. (2,0) should, based on these calculations, not give any resonance problems. (4,0) is at 1825 Hz in modal analysis. The RSI frequency is given by $302,4 * 6 = 1814,4$ Hz and this frequency could possibly get into resonance with the natural frequency. Operation at other loads than BEP would induce other RSI frequencies which could potentially create resonance problems. The natural frequencies obtained in this report shows mixed conformity. Results from the numerical simulations are within reasonable error margins, but the fact that the harmonic response analysis gives higher frequencies in water than the modal analysis is strange and undermines the trust of the implementation of damping in the simulations. Experimental results in air are only matched for (2,0).

From these numerical simulations, all the natural frequencies of the pump-turbine is not possible to obtain within certain margins of error. Operating turbines are experiencing more complicated boundary conditions and excitation forces, compared to this numerically studied pump-turbine. Further investigation should be conducted to determine the natural frequencies.

In my project thesis I worked with the natural frequencies of a circular disk. Results from the experiment in air showed good conformity with numerical simulations (deviations of ± 2 %). The experimental and numerical results in this report shows greater deviations. Based on my experience there is a big difference between a circular disk and a real turbine. The complicated geometry and boundary conditions clearly hampers the task of correctly calculating the natural frequencies. Adding flowing water, nearby walls and more realistic excitation forces will complicate it even more. Based on the results of this report, structural-acoustic simulation of complicated submerged structures can not guarantee a correct answer. Other sources of information should be used to confirm the numerical results.

By working with natural frequencies of this pump-turbine runner, the complexity of the machine and the calculations have become apparent. The runner is made from several parts welded together, each with its own natural frequencies. Each blade have the possibility to be excited with a force at resonance frequency. In addition, there are many other phenomena which are capable of causing pressure pulsations. The solution to the problem of fatigue damage in turbine runners may be more complex than that of being able to calculate the natural frequencies of the structure.

9 FURTHER WORK

Even though much effort has been put into solving the problem and many reports find good agreement between numerical and experimental results, turbines continue to break down after short time in operation. Generally, the aim should be to create models that better replicate the operating conditions of a turbine. This includes the investigation of close wall behavior and the impact on the added mass effect and FRR. Another interesting field of study is the influence of flowing water on the natural frequencies and the effect of rotation. Rotation of the turbine adds rigidity just like a spinning top. Both centrifugal and gyroscopic resistance forces will oppose movement and add stiffness to the structure (even if Presas et al (2014) [16] does not find any big impact of rotation). This could impact the natural frequency of the runner. The influence of small damages on the turbine could be investigated. Often, turbines will have some sort of imperfections. It could be manufacturing faults, sediment erosion or cavitation damage created by several years of operation. How do these damages alter the frequency response of a turbine and its ability to withstand resonance phenomena? With computers gradually getting more powerful, new and more detailed models can be developed. By utilizing simulations of models which more accurately replicate the operating conditions of a real turbine, important information on the vibration behavior can be gained. Even if numerical simulations can give important contributions to the construction process of a turbine, full scale experiments and experienced constructors and operators will still be of big importance.

The fact that not all researchers believe that resonance with the natural frequencies of the turbine is causing the breakdowns (ref Brekke (2010) [1]) and instead is blaming other effects, should be taken seriously. There are several harmonically varying forces, beside the RSI, in a turbine runner. When they coincide resonance could occur. Maybe the breakdowns are not caused by one factor only, but rather that each turbine is experiencing damaging fatigue loads from one of a series of different sources, each needing its own local fixes. The building strength of new turbines should also be investigated. Problems with fatigue damage have risen significantly in the last decades, in the mean time new and lighter turbines have been set in operation. The turbines might have become too fragile to withstand the fatigue loads experienced during modern day-operation.

REFERENCES

- [1] Hermod Brekke, *A Review on Oscillatory Problems in Francis Turbines*, Vannkraftlaboratoriet NTNU, 2010
- [2] C.G. Rodriguez, E. Egusquiza, X. Escaler, Q.W. Liang, F. Avellan, *Experimental investigation of added mass effects on a Francis turbine runner in still water*, Journal of Fluids and Structures 22, pages 699-712, 2006
- [3] Q.W. Liang, C.G. Rodriguez, E. Egusquiza, X. Escaler, M. Farhat, F. Avellan, *Numerical simulation of fluid added mass effect on a Francis turbine runner*, Computer & Fluids 36, pages 1106-1118, 2007
- [4] C.G. Rodriguez, P. Flores, F. G. Pierart, L. R. Contzen, E. Egusquiza, *Capability of structural-acoustical FSI numerical model to predict natural frequencies of submerged structures with nearby rigid surfaces*, Computer & Fluids 64, pages 117-126, 2012
- [5] Article from Teknisk Ukeblad, "<http://www.tu.no/kraft/2012/03/26/resonansproblemer-stoppet-svartisen-turbin>", Retrieved 29.09.14
- [6] Article from Teknisk Ukeblad, 2012 "<http://www.tu.no/kraft/2012/03/26/lopehjulet-sprak-i-svartisen>", Retrieved 17.06.15
- [7] Article from Wikipedia "[https://en.wikipedia.org/wiki/Tacoma_Narrows_Bridge_\(1940\)](https://en.wikipedia.org/wiki/Tacoma_Narrows_Bridge_(1940))", Retrieved 17.06.15
- [8] B. Hübner, U. Seidel, S. Roth, *Application of fluid-structure coupling to predict the dynamic behavior of turbine components*. IOP Conf. Series: Earth and Environmental Science 12, 2010
- [9] T. Chirag, G. Bhupendra, M. Cervantes, *Effect of Transients on Francis Runner Life: A Review*. J. Hydraulic Res. 51(2), pages 121-132, 2013
- [10] Einar Kobro, *Measurement of Pressure Pulsations in Francis Turbines*. Doctoral thesis, NTNU, 2010
- [11] D Valentin, A. Presas, E. Egusquiza, C. Valero, *Experimental study on the added mass and damping of a disk submerged in a partially fluid-filled tank with small radial confinement*, Journal of Fluids and Structures, 2014
- [12] Second order differential systems, notes from MIT "<http://ocw.mit.edu/courses/mechanical-engineering/2-003-modeling-dynamics-and-control-i-spring-2005/readings/notesinstalment2.pdf>", Retrieved: 05.10.14
- [13] M. Flores, G. Urquiza, J. M. Rodriguez *A Fatigue Analysis of a Hydraulic Francis Turbine Runner*, World Journal of Mechanics 2, pages 28-34, 2012
- [14] P. Bhatt, *Maximum Marks Maximum Knowledge in Physics*. Allied Publishers, ISBN 9788184244441, 2008
- [15] E. Egusquiza, C. Valero, X. Huang, E. Jou, A. Guardo, C. Rodriguez *Failure investigation of a large pump-turbine runner*. Engineering Failure Analysis 23, pages 27-34, 2012
- [16] A. Presas, D. Valentin, E. Egusquiza, C. Valero, U. Seidel *Experimental analysis of the dynamic behavior of a rotating disk submerged in water*, 2014
- [17] D. Valentin, A. Presas, E. Egusquiza, C. Valero *Influence of the added mass effect and boundary conditions on the dynamic response of submerged and confined structures*, 2014
- [18] Hiroshi Tanaka *Vibration Behavior and Dynamic Stress of runners of Very High Head Reversible Pump-turbines*, 1991

- [19] S. Lais, Q. Liang, U. Henggeler, T. Weiss, X. Escaler, E. Egusquiza *Dynamic Analysis of Francis Runners – Experiment and Numerical Simulation*, 2009
- [20] E. Egusquiza, C. Valero, Q. Liang, M. Coussirat, U. Seidel, *Fluid added mass effect in the modal response of a pump-turbine impeller*, 2009
- [21] Modes of vibration, UBC (University of British Columbia) "<http://www.theory.physics.ubc.ca/341-current/modes.pdf>", Retrieved: 07.10.14
- [22] ANSYS 15 Help Path: // Mechanical APDL // Theory Reference // Acoustics // Acoustic Fluid-Structural Interaction (FSI) Retrieved: 29.05.15
- [23] ANSYS 15 Help Path: // Mechanical APDL // Element Reference // Elements for Multiphysics Analysis // Elements for Acoustic Analysis // 3D Acoustics Element Usage Retrieved: 29.05.15
- [24] ANSYS 15 Help Path: // Mechanical APDL // Basic analysis guide // 5. Solution // 5.2 Types of solvers // 5.2.1. The sparse direct solver Retrieved: 14.06.15
- [25] A. Gahtak *Optics*, Tata McGraw-Hill, page 6.10, ISBN 978-0-07-058583-6, 2005
- [26] Wikipedia "http://en.wikipedia.org/wiki/Structural_analysis", Retrieved: 11.03.15
- [27] C. Q. Howard, B. S. Cazzolato *Acoustic Analyses Using Matlab and Ansys*, CRC Press, ISBN 9781482223279, 2015
- [28] ANSYS Inc. *ANSYS Mechanical APDL Theory Reference*, 2015
- [29] Wikipedia "http://en.wikipedia.org/wiki/Finite_element_method", Retrieved: 16.03.15
- [30] Wikipedia "http://en.wikipedia.org/wiki/Structural_acoustics", Retrieved: 16.03.15
- [31] Weidlinger Associates Inc "file:///C:/Users/omfjeld/Downloads/cipolla_-_weidlinger_-_computational_structural_acoustics_presentation.pdf", Retrieved: 16.03.15
- [32] O. de Weck, I. Y. Kim - Massachusetts Institute of Technology (MIT) "web.mit.edu/16.810/www/16.810_L4_CAE.pdf", Retrieved: 16.03.15
- [33] S. Moaveni *Finite Element Method*, 2013 Prentice Hall ISBN 0137850980,
- [34] F. Dompierre, M. Sabourin *Determination of turbine runner dynamic behaviour under operating condition by a two-way staggered fluid-structure interaction method*, 2010
- [35] W.R. Zhu, R.F. Xiao, W. Yang, J. Liu, F.J. Wang *Study on stress characteristics of Francis hydraulic turbine runner based on two-way FSI*, 2012
- [36] L. S. Chan, City University of Hong Kong "<http://personal.cityu.edu.hk/~bsapplec/natural.htm>", Retrieved: 17.04.15
- [37] Y. Wu, S. Li, S. Liu, H.S. Dou, Z. Qian *Vibration of Hydraulic Machinery*, 2013 Springer ISBN 978-94-007-6422-4
- [38] G. Olimstad *Characteritics of Reversible-Pump Turbines*, Doctoral Thesis, NTNU 2012
- [39] S. T. Haga *Dynamic load on High Head Francis turbines during start/stop*, Master Thesis, NTNU 2014
- [40] X. Escaler, J. K. Hütter, E. Egusquiza, M. Farhat and F. Avellan *Modal behavior of a reduced scale pump-turbine impeller. Part 1: Experiments*, 2010